TRANSMISSION ELECTRON MICROSCOPY STUDIES OF $LaMnO_3$ AND $La_{1-X}Sr_XMnO_3$ THIN FILMS GROWN ON VARIOUS SUBSTRATES

by

YINSHENG FANG

Presented to Faculty of the Graduate School of

The University of Texas at Arlington in Partial Fulfillment

of the Requirements

for the Degree of

MASTER OF SCIENCE IN MATERIALS SCIENCE AND ENGINEERING

THE UNIVERSITY OF TEXAS AT ARLINGTON

May 2010

ACKNOWLEDGMENTS

I would like to express my appreciation to Professor E.I. Meletis for his guidance and encouragement throughout this work. I would also like to thank Dr. J. C. Jiang for his instruction for the TEM sample preparation and analysis of TEM and HRTEM observation.

I wish to thank Dr. Hongquan Jiang for his help during deposition of films using the RF sputtering and guidance during XRD measurement and analysis and fruitful discussions.

I would like to thank Mr. Varad R. Sakhalkar for his cooperation and kind suggestion for the film deposition.

I also thank Ms. Jie He for her great help and encouragement in the TEM and HRTEM study.

April 16, 2010

ABSTRACT

TRANSMISSION ELECTRON MICROSCOPY STUDIES OF $LaMnO_3$ and $La_{1-x}Sr_xMnO_3$ THIN FILMS GROWN ON VARIOUS SUBSTRATES

Yinsheng Fang, M.S.

The University of Texas at Arlington, 2010

Supervising Professors: Efstathios I. Meletis and J. C. Jiang

$LaMnO_3$ (LMO) and $La_{1-x}Sr_xMnO_3$ (LSMO) thin films with colossal magnetoresistance have attracted considerable interest for potential applications in many technological devices, such as magnetic sensors and read-head of computer memory. In this work, polycrystalline and epitaxial LMO and LSMO thin films were deposited on various substrates including (001) Si, (001) MgO, and (001) $LaAlO_3$ (LAO) using RF magnetron sputtering. The microstructures of the thin films were initially studied using X-ray diffraction. Detailed microstructure information such as crystallite of the films, grain size, epitaxial quality, crystallographic structure and film/substrate interface were studied using high-resolution transmission electron microscope (HRTEM). More specifically, Effects of sputtering temperature, power and various substrates on the microstructure of the LMO and LSMO films were studied. HRTEM results showed that LMO and LSMO thin films on Si, MgO and LAO substrate deposited at 700 °C have (1) an amorphous structure using a power of 50 W and small crystalline structures using a power of 80 W. LMO and LSMO thin films on Si substrates deposited at 750 °C using a power of 30 W show nano columnar polycrystalline structures. By optimizing the deposition conditions, epitaxial LMO and LSMO thin films with a single crystal structure have been usefully fabricated on both LAO and MgO substrates at 750 °C using a sputtering power of 30 W.

TABLE OF CONTENTS

ACKNOWLEDGEMENT……iii

ABSTRACT……iv

LIST OF ILLUSTRATIONS……vii

LIST OF TABLES……x

Chapter Page

1. INTRODUCTION……1

2. OBJECTIVES……4

3. BACKGROUND AND LITERATURE REVIEW ……5

3.1 Perovskite Oxides ……5

3.2 Perovskite Lanthanum Manganite……7

3.2.1 Electronic Structure ……7

3.2.2 Jahn-Teller Effect……8

3.2.3 Double Exchange……8

3.2.4 Magnetoresistance……9

3. 3 Thin Film Growth……10

3.3.1 Growth Mechanism of Thin Films ……10

3.3.2 Polycrystalline Films ……10

3.3.3 Epitaxial Films ……11

3.4 Substrate Effects ……12

3.5 Previous Studies on Managnites Films……13

3.5.1 Maganite Films deposited by Pulsed Laser Deposition (PLD)……13

3.5.2 Maganite Films Deposited Using Chemical Vapor Deposition……14

3.5.3 Manganite Films Deposited by RF Sputtering……15

4. EXPERIMENTAL……16
4.1 Synthesis of LMO and LSMO Thin Films……16
4.1.1 Hybrid Plasma Assisted Sputtering System ……16
4.1.2 Experimental Materials……18
4.1.3 Procedures for LMO and LSMO Films Deposition……19
4.2 Microstructure Characterization ……21
4.2.1 X-ray Diffraction……21
4.2.2 TEM Study……21
4.3.3 Atomic Force Microscopy……23
4.3.4 Energy Dispersion Spectroscopy……23
5. RESULTS AND DISCUSSIONS……25
5.1 LMO Thin Films on Si Substrate……25
5.1.1 LMO Films Deposited at 700°C, 50 W……25
5.1.2 LMO Thin Film on the Si Substrate Deposited at 700 °C 80 W……27
5.1.3 LMO Thin Film on the Si Deposited at 750°C……31
5.2 Epitaxial LMO Thin Films on (001) MgO Substrate……35
5.2.1 Surface Properties by AFM……35
5.2.2 X-RAY Diffraction……37
5.2.3 TEM Analysis……38
5.3 Epitaxial LSMO Thin Films on (001) MgO Substrate……42
5.3.1 Surface Properties by AFM……43
5.3.2 XRD Analysis……44
5.3.3 LSMO films Analysis by Low Magnification of TEM……45
5.4 Epitaxial LMO Thin Films on (001) LAO……48
5.4.1 Surface Properties by AFM……49
5.4.2 XRD Analysis……49

5.4.3 Conventional TEM of LMO Films on LAO……..50

5.4.4 Interface Study by HRTEM……..52

5.5 Epitaxial LSMO Thin Films on (001) LAO Substrate ……53

5.5.1 AFM Analysis……53

5.5.2 XRD Analysis……54

5.5.3 *TEM Analysis*……54

5.5.4 Interface analysis of LSMO films on LAO by HRTEM……..56

5.6 Magnetic Properties……57

5.7 EDS Analysis ……59

6. CONCLUSIONS ……..61

REFERENCES ……..62

BIOGRAPHICAL INFORMATION……65

LIST OF ILLUSTRATIONS

Figure Page

3.1 Crystal structure of perovskite oxides……..……5

3.2 The orbital of Mn-ion in octahedral site……...7

3.3 Double exchange mechanisms.....……..8

4.1 Schematic illustration of the home built hybrid plasma PVD system……16

4.2 Side view of sputtering system.....17

4.3 Inner view of the used sputtering system……..……..18

4.4 Schematic illustration of basic steps to prepare TEM samples…….....23

5.1 Cross-section HRTEM of LMO/Si at 700°C using 50 W……...26

5.2 SAED pattern of LMO film and Si substrate deposited at 700°C using 50 W…….....26

5.3 HRTEM image of LMO/Si interface for films deposited at 700°C,50 W…….....27

5.4 XRD of LMO film on Si deposited at 700°C,80 W……28

5.5 XTEM image of the LMO/Si deposited at 700°C 80 W…..……..……29

5.6 SAED pattern of the LMO film and Si deposited at 700°C,80 W……29

5.7 Cross-section HRTEM LMO film on Si at 700°C using 80 W……...30

5.8 HRTEM image of the upper layer of the LMO film on Si deposited at 700°C 80……..31

5.9 XRD of the LMO film on Si deposited at 750°C ……..32

5.10 Cross-section TEM image of LMO/Si deposited at 750°C…….....……...33

5.11 Plane view TEM Image of LMO film deposited at 750°C and the corresponding SAED pattern (inset)……..……...…..33

5.12 XHRTEM image LMO/Si deposited at 750°C…....……...34

5.13 HRTEM image of a plan view LMO film on the Si deposited at 750°C.....35

5.14 NCM AFM 2D, 3D image of LMO/MgO……..…37

5.15 XRD of a LMO film on MgO deposited at 750°C.....……....38

5.16 TEM image of LMO on MgO deposited at 750°C, 30 W……..39

5.17 [100] zone SAED pattern of LMO film on MgO deposited at 750°C……...39

5.18 HRTEM image of a cross section LMO/ MgO deposited at 750°C……41

5.19 HRTEM image of cross section TEM of LMO/MgO deposited at 750°C…….....42

5.20 (a), (b) NCM AFM 2D, 3D image of LSMO/MgO……...43

5.21 XRD of LSMO on MgO deposited at 750°C…….....…44

5.22 TEM image of LSMO film on MgO substrates at 750°C……...45

5.23 (a), (b) b [100] zone SAED taken from the interface and substrates, respectively of the XTEM of LSMO films on MgO……..……46

5.24 HRTEM image of LSMO film on MgO substrate at 750 °C……..46

5.25 HRTEM image of LSMO film on MgO substrates at 750 °C .....……47

5.26 (a), (b) AFM NCM 2D, 3D image of LMO/LAO films ……49

5.27 XRD of LMO film grown on LAO substrate deposited at 750°C, 30 W……..50

5.28 TEM image (a) and SAED pattern (b) taken from interface between the LMO/LAO cut from the direction 1……..…....51

5.29 (a) cross section TEM observation of LMO/LAO and (b) [100] zone SAED pattern of interface from direction perpendicular to the direction 2 R D of LMO film grown on LAO substrate at 750 °C, 30 W……..…….51

5.30 HRTEM image of cross section of LMO/LAO……...…..52

5.31 (a) (b) AFM NCM 2D, 3D image of LSMO/LAO……..……..53

5.32 x-ray diffraction pattern of LSMO thin film on the LAO substrate.....……54

5.33 Cross section TEM image of LSMO film on LAO…….....…54

5.34 a SAED pattern taken from interface between LSMO and LAO, b, SAED pattern taken from substrate LAO at (100) zone axis…….....…....55

5.35 HRTEM image of cross section TEM of LSMO/LAO……..56

5.36 Typical hysteresis loop obtained from a sample at room temperature……..57

5.37 Hysteresis Loop for LMO thin films deposited on Si, MgO and LAO at 10K……..58

5.38 Hysteresis Loop for LMO thin films deposited on Si, MgO and LAO at 100K…….58

LIST OF TABLES

Table Page

4.1 Physics properties and crystal structure of the experiment materials ……..19

4.2 LMO and LSMO thin film deposition conditions……..20

5.1 Misfit between the films and substrate……..36

5.2 Composition of the selection LMO sample……..60

CHAPTER 1

INTRODUCTION

Perovskite manganese oxide thin films have been attracting increasing interest after the discovery of colossal magnetroresistance (CMR) in 1990s. The magnetic and electronic properties of lanthanum manganites have been intensely investigated as they are potential candidates for magnetic field sensors, non-cooled infrared detector and magnetroresistive read detectors. Thin films of lanthanum manganites are the most suitable for practical applications [1-3].Pure lanthanum manganite, $LaMnO_3$ (LMO), is cubic perovskite structure with lattice parameter a=0.391 nm [4], in which La atom sits at cube corner positions, Mn atom sits at the body centre position and the oxygen atoms sit at the face center [5][6].

Pure lanthanum manganite is an insulating material at room temperature [7]. Doping of the LMO with general formula $La_{1-x}A_xMnO_3$ (where A represents the dopant) improves the electrical and magnetic properties [8]. The Mn 3d orbits and O 2p orbital in the doped LMO overlap to form an electrical active band. The electrical and magnetic properties are relative to a double change of electron coupled Mn^{4+} and Mn^{3+} ion [9] [10]. Doped level in LMO will change the Mn^{3+}/Mn^{4+} ratio which have important influence to their electrical and magnetic properties and crystallographic structure. For example, a Mn^{4+} content about 30% have the optimal value to achieve the maximum CMR effect and the highest curies temperature (T_c) [11]. A rhombohedral, an orthorhombic and a monoclinic phase can be formed in $La_{1-x}Sr_xMnO_3$ depending on the synthesis condition. By changing the doped content of Sr, the compound $La_{1-x}Sr_xMnO_3$ evolves from antiferromagnetic to a ferromagnetic structure [12].

The unit cell of LMO have a MnO_3 octahedral structure, because of the Jahn-Teller effect, the structure of the octahedral is not stable. It will lengthen along the z axis. LMO has simple cubic perovskite structure at high temperature (T>750°C) [13]. Based on this structure, surface

energy and polarization of LMO were the main parameters to influence their properties. LMO has orthorhombic structure at low temperature, in which Jahn-Teller effect play an important role by affecting the lattice distortion and material properties [14].

Substrate material is an important factor affecting thin films structure and physical properties such as the Curie temperature shift, interface dislocation and formation of nano columns. Lattice misfit between the film and the substrate leads to the stress which is a function of thermal energy [15]. Due to the various lattice constant of the substrates, selecting different substrate will produce either tensile stress or compressive stress on the films, which will give rise to different result on the structure of films [16]. Recently, we found that nano columnar structure of thin films, misfit dislocations at the interface between the film and substrate are closely related to the lattice misfits. Moreover, by manipulating deposition temperature, rate of solidification of precursor and the substrate clean process, we can control the rate of growth and process of the crystal growth to get better quality films. The magnetic properties of the LMO thin films are influenced by the microstructure which is further controlled by the deposition conditions. Microstructure investigation of the LMO and LSMO thin films are insignificant issues in the present work.

Fabrication of the high quality thin films is basely desirable requirement to carry out this research. LMO and doped LMO thin films are very expensive material and pulsed laser deposition (PLD)[15][16] is a good instrument to fabricate the all assorts of manganese oxides thin films. It was reported that polycrystalline and epitaxial thin films have successfully been fabricated by PLD, however it is well known that only small size can be made by this technique. A large scale thin film deposition method is necessary in order to utilize this material in commercial future applications. We need to explore a novel technique to manufacture it. Magnetron sputtering is the most suitable method to fabricate the thin films for a scale up and technological transfer from the lab to the industries of LMO and LSMO films whose advantages are low cost, easy operating, and large size and high quality. In the literatures, there are some researchers using the RF magnetron sputtering to synthesize the manganite thin films, most of process is to fabricate the

amorphous structure films first and then annealing the films to get the polycrystalline structure [17][18].

Recently, by manipulating the deposited conditions, we have successfully fabricated the single crystal LMO and LSMO films on both the LAO and MgO substrates. The polycrystalline LMO and LSMO have been demonstrated as the byproducts of this optimal process. We have not found any report on depositing single crystal LMO and LSMO thin films.

High resolution transmission electron microscope (HRTEM) can provide crystal lattice images, namely periodicity of crystal structure, and the information of atomic positions. This enables us to investigate not only bulk but also interfaces and lattice defects.

This work will present the achievement of single crystal LMO and LSMO thin films grown on various substrates, such as LAO, MgO, and Si with different orientations (100) and (111) using RF magnetron sputtering. I have also extensively investigated the microstructures of films created by other students using XRD, TEM and HRTEM.

CHAPTER 2

OBJECTIVES

Although numerous beneficial properties of manganite film are well known, a good understanding of mechanism of electronic and magnetic properties of manganite film has yet to be developed. Its microstructure can be extensively investigated by XRD; however, detail of microstructure of manganite film needs to be further understood. Parallel research work in the SaNEL laboratory LMO and LSMO films have been fabricated ref. (Varad Sakhalkar thesis)

Specifically, objective of the research are:

1) To study the polycrystalline and epitaxial LMO perovskite films on various substrate deposited by RF mode magnetron plasma assisted sputtering.
2) To study the characteristics of the nano columnar structure of the thin film using TEM, HRTEM.
3) To study the effect of deposition parameter on microstructure of Lanthanum manganite films.
4) To study the effect of substrates on the microstructure of Lanthanum manganite thin films.
5) To fabricate epitaxial LMO and LSMO thin films.

CHAPTER 3

BACKGROUND AND LITERATURE REVIEW

Lanthanum manganite attracts tremendous attention as a class of perovskite material for a lot of properties, such as colossal magnetoresistance, ferroelectricty, charge ordering, spin transport and all those properties associated with crystalline structure [19]. LMO is the foundation to study the perovskite manganite oxide and Sr-doped lanthanum mangananite attracted more attention in the decade for possessing CMR at room temperature [20]. To further understand the properties and structure of LMO and LSMO thin film; it is necessary to take an overview of the structure and properties of perovskite oxide material.

3.1 Perovskite Oxides

In 1839, Gustav Rose discovered perovskite mineral in the Ural Mountains of Russia and named it after Russian mineralogist, L.A. Perovskite [21]. Perovskite refers to a class of material which have the similar crystalline structure as calcium titanate which has the general formula ABX_3 where A and B are metallic cations and X is a nonmetallic anion. X is usually oxygen. A can be rare earth element, alkali element or other large ion. B can be transition metal ion located at octahedral site as shown Fig 3.01.

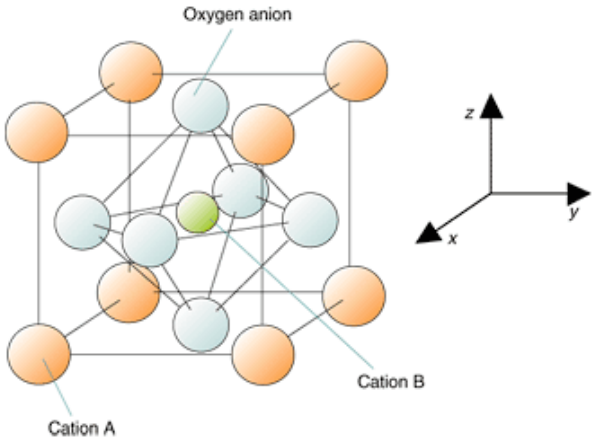

Figure 3.1 Crystal structure of perovskite oxide

Pure bulk perovskites are usually electrical insulators [22], because all of the atomic sites are occupied, and strong ionic bonds keep the atoms and their electrons in place making it difficult for electrons to freely move through the crystal. These compounds have cubic symmetry and are isotropic. It is established that the perovskite structure is only stable when the Goldschmidt tolerance factor t, defined by $t = \frac{(r_a + r_x)}{\sqrt{2}(r_b + r_x)}$ (r is the radii of the ions), approximately equals one. For example, if the A cation is too small in relation to the B cation, the octahedral will tilt and twist and the symmetry will be lowered. More interesting physics arises when there is some slight distortion of the perovskite structure. So it provides a method to design to adjust electrical, optical, elastic, magnetic and other physical properties. The result can be materials that are semiconducting, conducting or superconducting. Moreover, when the materials are prepared as thin films, the crystal structure and physical properties will be affected by the substrates. Thus, when deposited on the substrates, perovskite material thin films will indicate assorted of attracted electric and magnetic properties for the strain between the substrate and film. At the same time, the compound structures are related to the thickness of the thin films and corresponding to electrical and magnetic properties. When the films grow in thickness, because the strain in the film was relaxed at the upper layer, the compounds can be divided into different layers. J. C .Jiang and coworkers studied the LSMO films grown on LAO using PLD. The TEM observations revealed that LSMO films were separated into two layers, the layer adjacent to substrates were continuous and homogenous single crystal structure and upper layer was a nanopillar structure with the same orientation.

Another method of controlling the properties is to replace the cation sites with different atoms. For example, if the some amounts of La ions in LMO are replaced by Ca or Ag, the crystals have different CMR effects. W. Cheikh-Rouhou [8] studied the effects of silver doping upon the physical properties of LMO and found that silver doping led to a decrease of the unit cell volume and reduce the Curie temperatures. In this work, we have studied effect of Sr doping on the microstructure of LMO thin films.

3.2 Perovskite Lanthanum Manganite

3.2.1 Electronic Structure

$LaMnO_3$ is a significant ceramic material that belongs to perovskite structure and doped $LaMnO_3$ has stronger colossal magnetoresistance. To understand the mechanism of producing the CMR effect, it is necessary to know the electronic structure of the compound.

The unit cell of LMO consists of a MnO_6 octahedral, in which the Mn occupies the center position and 6 oxygen atoms occupy the corner site. The configuration of the outer orbit electron in the Mn ion is $3d^4$. Each manganite is surrounded by six oxygen ions, in an octahedral configuration. In 3d transition-metal oxides, the orbit degree of freedom has strong effect on the material electrical, magnetic and structural properties. Because of crystal field splitting, the five 3d orbital are divided into two sets which are e_g orbital and t_{2g} (Figure 3.2). The e_g orbits are oriented towards the neighboring oxygen while the t_{2g} states have nodes in these directions. This means that the e_g orbital can intermix with the oxygen p orbital.

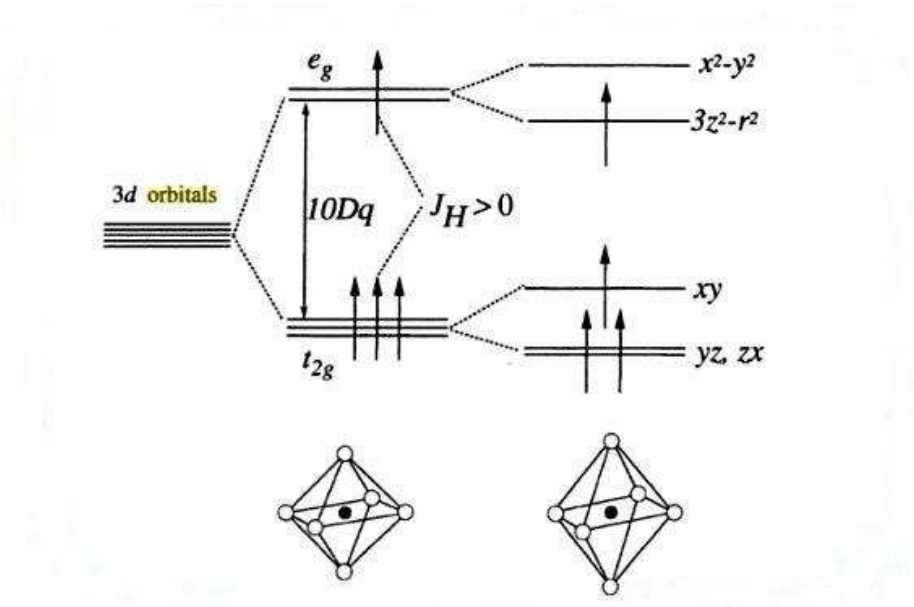

Figure 3.2 the orbital of Mn-ion in octahedral site

In a non-doped LMO compound, Mn ions are +3 valences and have one electron in the lower e_g orbits ($3z^2$-r^2). If an electron wants to move a Mn ion to another one, it has to go to a higher energy e_g level state (x^2-y^2), which is energetically unfavorable. Therefore, the non-doped LMO is an insulator. In a doped LMO with some 2 valance ions, such as Ca^{2+}, Sr^{2+}, some Mn ions change to Mn^{4+} of which the e_g lower orbit ($3z^2$-r^2) is empty and electrons can move to this empty orbit. A fully doped manganite is also an insulator because e_g carriers are completely empty.

3.2.2 Jahn-Teller Effect

The Jahn-Teller splitting of the outer Mn d level is considered to be related to electronic and magnetic properties and to the structure of LMO and doped LMO. Hermann Arthur Jahn and Edward Teller used group theory to prove that non-linear degenerate molecules are not stable. Electrons with degenerated electronic ground state will undergo a geometrical distortion to lower the overall energy of the complex. Jahn-Teller effect is very common in six coordinate manganese (III) complexes with octahedral structure. The Jahn-Teller effect causes the octahedral complexes to distort along fourfold axis (labeled as the z axis) by usually elongating the bonds along the z axis [31].

3.2.3 Double Exchange

A correlation between magnetic order and conductivity in the $La_{1-x}D_XMnO_3$ was found by Jonker (D being a divalent alkaline earth Ca, Sr, or Ba). These manganite alloys are insulating and antiferomagnetic at the x=0, or x=1, but ferromagnetic for the composition range 0.2<x<0.5.

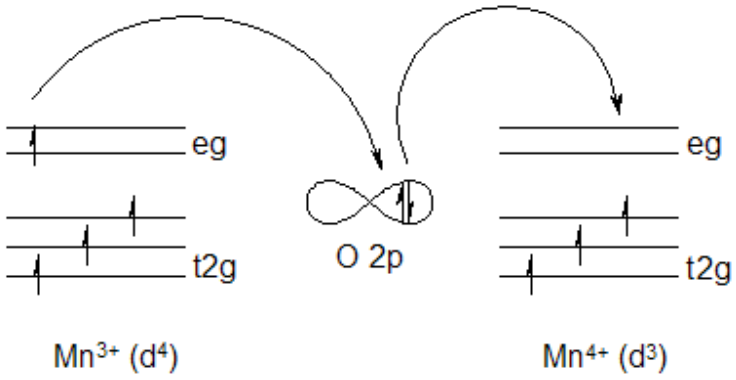

Figure 3.3 Double exchange mechanisms

In 1951 Zener proposed double exchange concept (Figure 3.3) to explain the correlation between the electrical conductivity and ferromagnetism [5]. Double exchange mechanism predicts that it will be relative easy for an electron to be exchanged between two species and has important implication for both ferromagnetic and antiferromagnetic materials. Considering in a 180 degree interaction of Mn-O-Mn, Mn e_g orbital electrons are directly interacted with O 2p orbital. Therefore, electron movement from one species to another will be easier if the electrons do not need to change spin direction. Namely, this double hoping electron requires that both hopping electrons have the same spin.

3.2.4 Magnetoresistance

In the1990s with the discovery of colossal magnetoresistance (MR) of LMO, the interest of perovskite manganite was fueled. Magnetoresistance is the property of a material to change the value of its electric resistance in an external applied magnetic field. The mobility of charge carrier depends on the magnetic environment. The effect was first discovered by William Thomason (more commonly known as Lord Kelvin) in 1856, but he was unable to lower the electrical resistance by more than 5%. This effect was later called ordinary magnetoresistance (OMR). More recent researchers have discovered materials showing giant magnetoresistance (GMR), colossal magnetoresistance (CMR) and magnetic channel effect (TMR).

The magnitude of the MR is usually defined as:

$$MR = (\rho_H - \rho_0)/ \rho_0$$

Where ρ_0 is resistivity at initial magnetic field and ρ_H is resistivity at a certain magnetic field.

It was established that the perovskite manganese oxide exhibits a transition from a ferromagnetic metal to paramagnetic insulator or semiconductor as increasing temperature accompanied by maximum in the electrical resistivity at the temperature Tp. The CMR effects will be produced near temperature $T_{p.}$ Sr doped manganite exhibits CMR at near room temperature which attracted tremendous interest in the past decade [6][7][8].

3.3 Thin Film Growth

3.3.1 Growth Mechanisms of Thin Films

Based on the thermal dynamic principle, there are two types of basic film growth on a flat surface, which are termed island growth and layer growth. The later is often subdivided into two modes: two dimensional layer-by-layer growth and layer-plus–island growth. In the last case the growth begins as a thin layer followed by developing islands and/or particles as growth proceeds. The growth process of material on a substrate can be divided into nucleation, coarsening, coalescence, grain growth, recrystalization and thickening.

The substrate surface structure such as steps, terraces and kinks plays an important for film nucleation and morphology. Nucleation was observed to occur on the surface terraces. The steps usually introduce defects such an anti-phase domain boundaries. While in the case of island growth mode, the characteristics of terraces have be a limiting factor for controlling the lateral crystallite size.

Epitaxial growth of thin films on a substrate initiate through the nucleation of isolated crystals on a substrate surface. Later these crystals further grow along the lateral direction in plane of the film. interphase. Coalescence is the result of the lateral growth resulting in the formation of boundaries. This defines the initial grain structure characteristics of film. Nucleation and coalescence result in formation of a film less than 10 nm but for most of the applications further thickening of the films is required. Grain structure evolution during thickening occurs in two fundamentally different ways. If the grain boundaries formed through impingement are immobile, the grain structure resulting from nucleation, growth and coalescence process is retained in the films. It should be noticed that it is important that the substrate do not undergo any transitions in the temperature range spanned from the preparation temperature to growth temperature.

3.3.2 Polycrystalline Films

Polycrystalline film refers to a class of films whose microstructure is crystalline, namely long-range ordering structure but contains random oriented crystals without any orientation preference. The microstructures of polycrystalline film have great influence on the electric and magnetic

properties of the films. These polycrystalline films are widely used in electronic device, all kinds of transducer and actuator. Currently, in reported papers, most of fabricated LMO films have polycrystalline structures [18][21][23]. For example, Kyung-ku et al. studied the microstructure and magnetoresistance of LSMO thin films and reported that polycrystalline LSMO films exhibited enhanced MR value in weak magnetic fields [14].

3.3.3 Epitaxial Films

Epitaxial growth is a typical process of depositing a single crystalline film on a single crystalline substrate. So the deposited film is called as an epitaxial film or epitaxy layer. Usually, epitaxial film may be grown from gaseous or liquid precursors. The substrate acts as a seed crystalline and the deposited film will imitate the structure and orientation of the substrate, namely, the structure and orientation of film will be identical to the substrate. There are two kinds of the films as deposited on a substrate, homoepitaxy and heteroepitaxy. Homoepitaxy is a special process in which the material of film is same as the material of substrate. This technology is used to fabricate more pure material than substrate or to make a layer having various doping levels. Heteroepitaxy is a process to grow thin films whose material is different from the substrate. If the lattice parameters of the film and the substrate are different, it produces a lattice misfit at the interface. This lattice mismatch plays an important role on the microstructures and the electric and magnetic properties of the as-grown films. Hetero-structures can produce important materials by combining semiconductor, metals, insulator, metal oxides and ferroelectrics. Currently, there are great developments in device applications and fundamental researches of artificial heterostructural materials due benefited from the fast development of fabrication and characterization technologies. In this work, we focused on the perovskite oxide heterostructures fabrication and microstructure characterization and studied growth temperature and substrate effects on the films microstructure and properties.

3.4 Substrate Effects

Substrate material is a very important factor which influences the microstructure and properties of manganite thin films. For example, strain in the film leads to the shift of Curie temperature. The strain is a function of the substrate thermal expansion and the mismatch between the substrate and the films. A large difference in thermal expansion coefficient of the substrate and film will result in cracking of the film when the temperature changes. Such thermal expansion coefficient mismatch maybe causes more problems for the brittle material film that is possible to break the film on the substrate. The thinner films might conform to the substrate in this situation whereas a thicker film would not.

Chemical reaction between the substrate and the film will make the deposited film unstable, which results in a change of the structure and properties of the film with time. Also there should not be any Reactions between the film and the substrate need to be avoided in the oxygen atmosphere to grow manganites.

A uniform surface is a basic requirement of the substrate in order to achieve a uniform homogeneous film because the deposited film structure initially imitates the structure of the substrate. Defects on the substrate surface have a significant impact on the nucleation of the film and accordingly on the film morphology and structure. If a substrate consists of a small amount of a phase other than the predominant one that might affect the surface, the films may not grow well on the whole substrate. According to nucleation theory, disoriented grains frequently nucleate on irregularities on the surface. The surface morphology not only affects the crystal the orientation but also influence the rate of crystal growth. Any defects on the substrate may produce similar defect in the films. Impurity phase inclusions and twins will likely affect the epitaxial quality. Twin boundaries that propagate throughout the substrate are potential nucleation sites for competing crystalline directions. Therefore, thin film deposition process need to work in a clean environment. In this work, the substrates were initially cleaned by acetone followed by argon plasma cleaning.

In order to grow epitaxial films there are more factors that should be considered. Epitaxial structure means that there is a definite orientation relationship between the films and the substrate. The difference between in-plane lattice parameters should be minimized to achieve epitaxial films. Differences in lattice parameters can also be a way of changing the properties of the film. In this work, we investigated the effect of the lattice misfit on the microstructure of LSMO and LMO films. It is clear that smaller misfits will get better films and larger misfits will decrease the epitaxial quality of the films. Furthermore, the atoms of the films that coincide should preferably have the same atomic size and valiancy with respect to the substrate. This means that a good substrate should have a similar structure to the film material.

When a film is grown, the first layer will be subjected to strong stress due to the misfit between the substrate and films. Increasing film thickness, the strain will relax through the appearance of misfit dislocations, and the film properties should approach those of the bulk material.

3.5 Previous Studies on Manganite Films

In the literature, manganites have several types of crystal structures including cubic, tetragonal, rhombohedra, and monoclinic. However, all these can be regarded as a distortion of the basic cubic perovskite structure with a=3.9Å. If there is a deviation from the Goldschmidt tolerance factor ideal value, the crystal will lower its symmetry and the new structure will be of some other type. A large misfit of the ionic sizes will distort the MnO_6 octahedral leading to an orthorhombic structure. In past ten years, extensive researches about manganite oxide materials have been about their properties, microstructures and methods of fabrication.

3.5.1 Manganite Films Deposited by Pulsed Laser Deposition (PLD)

TEM studies of the LSMO thin films on LAO substrate by J. C .Jiang *et. al.* [6] [7] showed that manganite films deposited by PLD at 700 °C under oxygen partial pressure of 400 mTorr were divided into two layers: a continuous layer adjacent to the substrate and a column layer grown on the continuous layer. A continuous layer has a cubic structure (a= 3.88 Å) and the columnar layer is composed of periodically arranged nano columns with an orthorhombic

structure (a=5.52 Å, b=5.56 Å, c=7.76 Å). The continuous LSMO layer is a single crystal structure with a $<100>_{LSMO}//<100>_{LAO}$ orientation relationship. LSMO nano columns exhibit an orthogonal shape and have a uniform grain sizes about 25 nm. The nano column boundaries showing an amorphous structure correspond to a highly strained and highly defective structure and the interface between the continuous layer and the column layer is nano column boundary's start point. The edge dislocations were also demonstrated at the film/substrate interface by HRTEM observation. The LSMO film on LAO deposited at 800 °C was greatly different from the films deposited at 700 °C. Nano column structure was not found in the film deposited at 800 °C, only the continuous single crystalline structure was observed.

G. Y .Wang [28] and coworkers reported $LaCaMnO_3$ films on (001) LAO under different oxygen partial pressures using PLD at 750°C. XRD and selected area electron diffraction (SAED) pattern showed that the film is well epitaxially grown. Phase separation was found in the films. Serious crystal defects are observed by HRTEM. H.S KIM tried to use DC reactive sputtering technique for LMO layer deposition. Deposition of LMO film on MgO by reactive DC sputtering at temperature of 850°C and Ar partial pressure of 1.3 x 10^{-3} pa (0.01 mTorr) was successful. Studies of XRD θ-2θ scan showed the XRD diffraction pattern only demonstrated two sharp peaks of plane (100) and plane (200) of LMO thin films indicating that the LMO film has a texture structure.

3.5.2 Manganite Films Deposited Using Chemical Vapor Deposition (CVD)

Patrick Herve TCHOUA Ngamou [4] and coworkers reported that manganite films were deposited on Si substrate at 700 °C using a growth rate 0.48 nm/min by CVD. XRD study shows that the films were polycrystalline in structure and have a grain size of about 57 nm. The crystallographic structure of LMO is rhombohedra (R-3c).

O. Yu. Gorbenko [11] reported that the $LaAgMnO_3$ film was deposited on the single crystal substrates (001) and (110) $SrTiO_3$, and (001) LAO by CVD at 800 °C. XRD and HRTEM studies revealed that the film has epitaxial quality. HRTEM studies also showed that low angle grain

boundaries between the film and substrate were also formed due to the lattice mismatch between the substrate and film.

3.5.3 Manganite Films Deposited by RF Sputtering

Kyun-ku [14] has reported the growth of LSMO thin films on single crystal (100) $SrTiO_3$ and (100) LAO substrate by RF sputtering at 650°C in a sputtering atmosphere of 60%Ar and 40%O_2. The XRD results indicate that (100) orientation preferred LSMO was obtained. TEM observations indicated the LSMO films had substrate-dependent grain size. Defects which are composed of large area with well crystallized feature and isolated mixture area were observed.

M-J. Casanove [21] studied LSMO manganites film deposited on (001) MgO by RF magnetron sputtering at 800- 900°C in a reactive plasma Ar (80%) –O_2 (20%) at 3.75 mTorr. LSMO films are epitaxially grown with an in-plane orientation relationship $[100]_{LSMO}//[100]_{MgO}$. There are slight disorientation between the LSMO and MgO. TEM observations suggested that there are dislocations networks in the film which are not regularly distributed with a mean spacing ranging from 100 to 300 nm and some needle-shaped crystalline domains present. Those dislocations network and needle shaped domain appearing in the LSMO film originate from the misfit between the substrate and the film.

CHAPTER 4

EXPERIMENTAL

Lanthanum manganite thin films are synthesized on various substrates including (001) Si, (001) MgO and (001) LAO using RF sputtering. The LMO, LSMO sputtering targets are obtained from Kurt J Lesker Company with 99.9% purity. All of the depositions were conducted using the home built hybrid CVD system. The details of the deposition system will be introduced in the following section.

4.1 Synthesis of LMO and LSMO Thin Films

Sputtering is a type of vacuum deposition system that uses energetic ions to knock atoms or molecules out from a target that acts as one electrode and subsequently deposit them on a substrate acting as another electrode

4.1.1 Hybrid Plasma Assisted Sputtering System

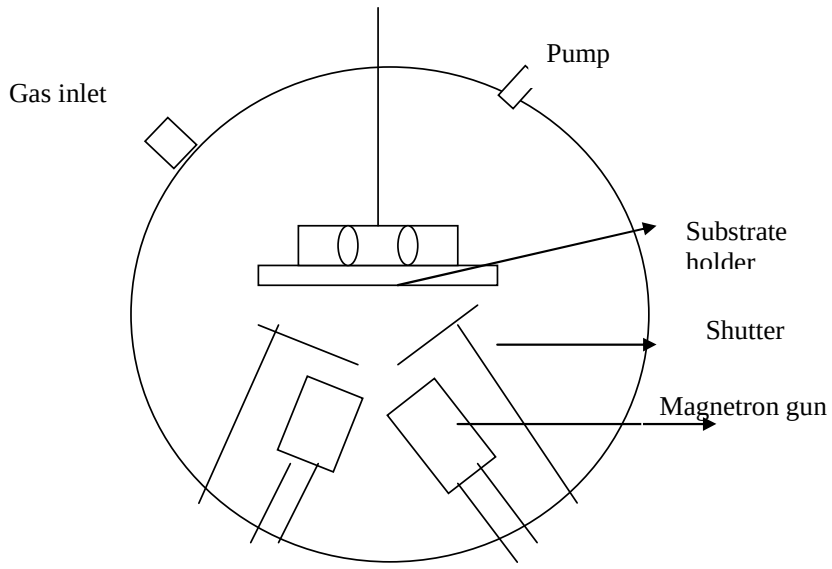

Figure 4.1 Schematic illustration of the home built hybrid plasma PVD system

Figure 4.1 demonstrates a schematic illustration of the hybrid plasma PVD system. Although there are huge developments in the technique of the sputtering, the principle of the fundaments is more or less the same. The target and the substrate are located in the chamber face to face serving as electrodes. Inert gas, typically, Argon with a pressure introduced into the system as the medium to initiate and maintain a glow discharge. When an electric field is applied to electrodes, glow discharge is initiated and maintained between electrodes. Free electrons will be accelerated by the electric field and gain sufficient energy to ionize argon atoms and the positive argon ions strike the electrodes resulting in ejections of neutral target atom through momentum transfer. The atoms deposit on the substrate at the opposite position.

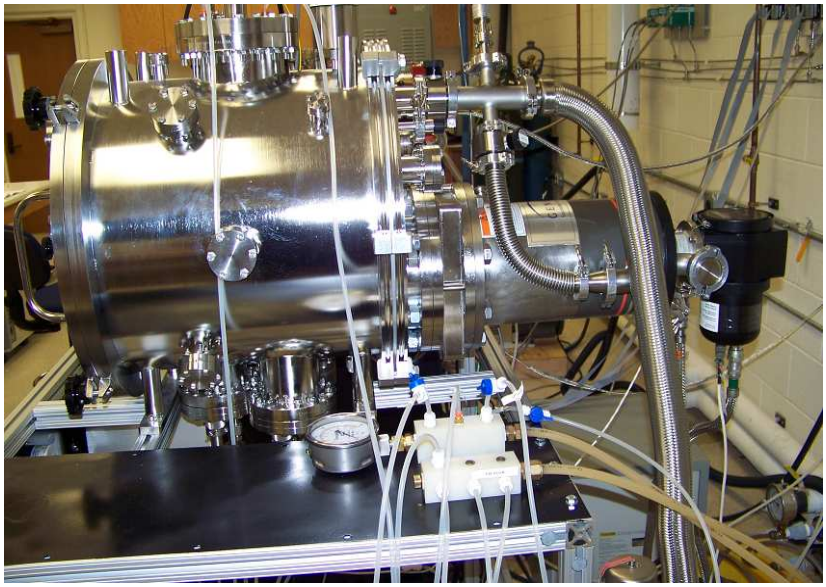

Figure 4.2 Side view of hybrid plasma PVD system

Film depositions were performed using an RF magnetron sputtering system with a stainless steel cylindrical chamber with 18.38 inch diameter and 19.66 inch length connected to a mechanical pump and cryo pump (Figure 4.2). The system was equipped with two 2-inch magnetron sputtering source positioned at a 30 degree inclination to the substrate center with a target to substrate distance of 150 mm (Figure 4.3). This system has both DC and RF biasing capabilities. Substrates were kept at a constant temperature during the deposition using lamp

heating on the backside of the alloy plate using an automatic temperature control unit. The deposition system was evacuated to a background pressure down to 3~5 x 10^{-6} Torr and pure gases of Ar (99.99%) with required quantity were introduced through mass flow controllers to fill to required pressures for the deposition.

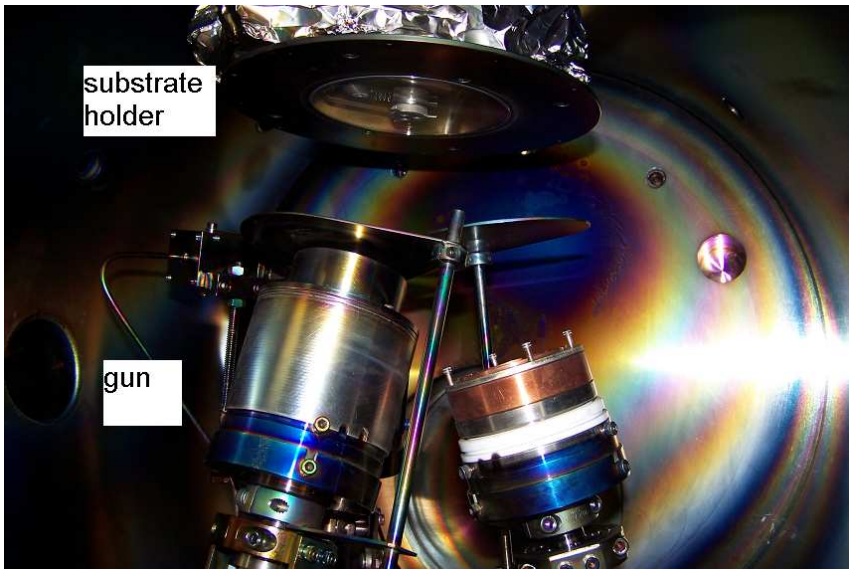

Figure 4.3 Inner view of the sputtering system showing
two sputtering guns and the substrate holder

During deposition, very precise pressure control is maintained using an automatic gate valve in conjunction with an MKS 146C PID controller. The thermocouple gauge is used to measure the roughing line pressure. The ion gauge measures the pressure when the chamber is exposed to the cryo pump for creating high vacuum. It operates only below 10^{-4} mTorr.

4.1.2 Experimental Materials

Target materials LMO and LSMO (purity 99.9%) were supplied by Kurt J. Jesker Company Substrate LAO (Lanthanum Aluminate) single crystal has a lattice constant (0.3790 nm), proper dielectric constant and low dielectric loss in microwave band; it is used for high T_c microwave electronic devices (for example high T_c superconductive filter in mobile communication). It has been widely applied in the communication industry. MgO (Magnesium Oxide) substrate is widely used for various films: magnet film, semi conductive film, optical film as well as high T_c

superconductive film. MgO crystal has low dielectric loss in microwave band, so it is an important material for high T_c superconductive microwave devices in the mobile communication as well as other industrial areas. The physical properties and crystal structure information of the materials are listed in Table 4.1, as shown in the following.

Table 4.1 Physics properties and crystal structure of the experiment materials

	Substrates			Films
	$LaAlO_3$	MgO	Si	LMO_3
Crystal structure	Pseudo cubic	Cubic	Cubic	Cubic
Melting temperature	2373 K	3250 K	1683.15 K	N/A
Density	6.52 g/cm^3	3.58 g/cm^3	2.329 g/cm^3	N/A
Specific heat	0.427 J/g.K (298 K)	0.879 J/g.K (298 K)	0.7 J /gK	N/A
Thermal conductivity	9W/m. k (300k)	59 W/m.k (300 K)	130 W /mK	N/A
Thermal expansion	11.6 x 10^{-6} K^{-1} (300 K)	11 x 10^{-6} K^{-1} (300 K)	2.6·10^{-6} K^{-1}	N/A
Lattice parameter	0.379 nm	0.4213 nm	0.5431 nm	0.391 nm

4.1.3 Procedure for LMO and LSMO Films Deposition

LMO and LSMO films were deposited on the Si (100) p-type wafers and single crystal MgO (100) and LAO (100) by magnetron sputtering. Thin films deposited on Si substrate used in this work were prepared by Mr. Varad R. Sakhalkar in the same lab and the deposition of these films was not repeated in this work. The fabrication part of this work focuses on the epitaxial LMO and LSMO thin films growth on LAO and MgO substrates.

Two deposition methods were used in this work. Specially:

Method I: Prior to the deposition, substrate surface were cleaned in acetone for 10 minutes followed by alcohol to remove residual acetone. The substrates were then dried up with compressed air. A standard procedure to eliminate contaminant in the chamber and on the

substrates is as follows: Initially, the chamber was pumped down to 10 mTorr using the mechanical pump and then the cryo pump to obtain a vacuum level of about 2-3 x10^{-6} Torr. The chamber was filled the Ar (99.9%) gas to remove air in the gas line and then pumped down to pressure about 2-3 x10^{-6} Torr again. The cleaning of substrate surface were performed using RF sputtering at 750 °C using a power of 30 W for twenty minutes to remove the surface contaminants.

Method II: The substrates were not cleaned by acetone and were used as is from the supplier. The argon plasma was performed to clean the substrate for 10 min at 10 mTorr with 30 W RF power. Then the substrate was heated up to 750 °C and kept at this temperature for 20 min to enable the surface reconstruction and recover from the damage of argon plasma. After the substrate temperature reached to 750 °C, the sputter gun was turned on with the shutter closed for target cleaning. The deposition started when the shutter was opened. The deposition lasted for 4 hours.

Table 4.2 LMO and LSMO thin film deposition conditions

Sample	Substrate	Sputtering pressure (mTorr)	FILM	Substrate temperature (°C)	RF power (W)	Deposition time(h)
LMO-Si1	Si	10	LMO	750	30	3
LMO-Si2	Si	10	LMO	750	50	2
LMO-Si3	Si	10	LMO	700	50	1
LMO-Si4	Si	10	LMO	700	80	1
LMO-M1	MgO	10	LMO	750	30	2
LMO-L1	LAO	10	LMO	750	30	3
LSMO-M1	MgO	10	LSMO	750	30	2
LSMO-L1	LAO	10	LSMO	750	30	4

4.2 Microstructure Characterization

The characteristics of crystalline structure determine all kinds of the properties of perovskite materials. Observation of the microstructure is an effective method to understand and analyze fundamental properties associated with the microstructure. Transmission electron microscopy (TEM) and high-resolution (HR) TEM are powerful tools to examine the microstructure for their high resolution and electron diffraction technique to determine the orientation of the crystal. XRD is another effective method to characterize the structure of the crystalline whose advantages are ease of operation and without need to destroy the samples. In this work, after we deposited LMO, LSMO thin films on (001) LAO and (001) MgO substrates using RF mode magnetron sputtering, we used XRD to have a quick investigation of the thin film quality. For high quality films, we proceed to use the TEM to further study the microstructure of the thin films. X-ray diffraction measurements were conducted in a SIEMENS D500 diffractometer operating at 40 kV and 30 mA. Plane view and cross-section TEM studies were conducted in a JEOL 1200 EX microscope operating at 120 kV and a Hitachi H-9500 HRTEM operated at 300 kV.

4.2.1 X-Ray Diffraction (XRD)

Siemens D-500 Diffractometer is equipped with Cu K_α x-ray radiation source (wavelength 1.54 Å) and Ni filter. Θ-2Θ diffraction was used for the investigation. X-rays are incident upon the sample making an angle (θ). If the Bragg reflection occurs, there will be a reflection at an angle 2θ relative the incoming beam. In another words, the x-ray source is fixed, sample moves through the θ –angles by title the sample, and X ray detector moves with twice the angler speed of the sample, keeping 2 θ angles.

4.2.2 TEM Study

TEM is an effective method for investigating materials especially for nanostructures. TEM observations can lead to the discovery of new materials and structures. Plane view and cross section TEM observation are two commonly methods. Cross section TEM observation can obtain important information of the interface between the substrate and the film which closely relate to the mechanism of crystal nucleation, growth, and defect and strain, as well as the orientation

relationship. One of the difficult issues in using TEM is sample preparation for the thin film specimens. The following lists the basic cross-section and plan-view TEM sample preparation procedures (Figure 4.4).

4.2.2.1 Method for Cross-Section TEM Sample Preparation

1. Cut two rectangular pieces of material about 3x3 mm from the sample along a specific direction using diamond saw.
2. Glue these two pieces face to face by joining the film side using 610 adhesive.
3. Cut the adherent piece into the slices 1x3 mm
4. Polishing the sample on the cross section side sequentially conducted on diamond lapping films with 30, 9, 3, and 0.5 μm.
5. Mount the sample on support copper ring and then grind using 1200 grit sand paper to reduce the thickness of the sample.
6. Place the sample on a precision dimple grinder and polish the sample using Cu wheel and fine diamond paste.
7. Using an ion mill to reduce the sample thickness until there are hole produced close to the film.

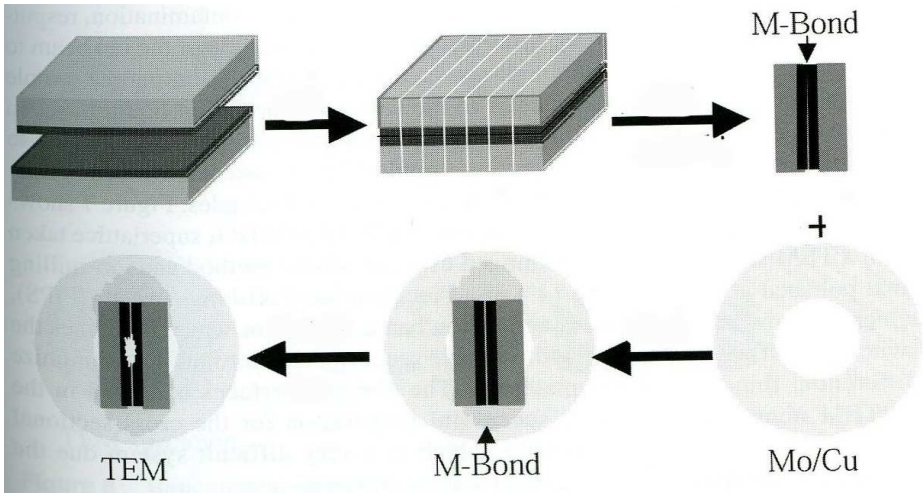

Figure 4.4 Schematic illustration showing basic steps to prepare cross-section and plan-view TEM samples

4.2.2.2 Method for Plane View TEM Specimen Preparation

1. 1 Cut a piece of sample 2x2 mm using the diamond saw.
2. Stick the sample on the copper ring using the films side down.
3. Polish samples using the 1200 grit sand paper.
4. Place the sample on a precision dimple grinder and polish the sample using Cu wheel and fine diamond paste.
5. Use the ion mill to reduce the sample thickness.

4.3.3 Atomic Force Microscopy (AFM)

Selected samples were used for the surface morphology and roughness investigation using a Park System XE-70 Atomic Force microscope imaging with a non contact mode. In non contact mode, the tip does not contact the surface of the sample, and the oscillation frequency of cantilever is slightly above resonant frequency, where the amplitude of oscillation is about a few nanometers. The Van Der Waals force which is greatest at this distance acts as a damped force.

4.3.4. Energy Dispersion Spectroscopy (EDS)

EDS is used to study the chemical composition of the LMO thin film. EDS system is attached to a JEOL JSM-6100 Scanning Electron microscopy (SEM). The accelerating voltage 20 kV and a work distance of 15 mm were used for EDS analysis.

CHAPTER 5

RESULTS AND DISCUSSIONS

5.1 LMO Thin Films on Si Substrate

LMO films on Si substrates at various substrate temperatures and supply powers were fabricated. The variation of deposition parameters results in different quality of the as-deposited thin films.

5.1.1 LMO Films Deposited at 700℃, 50 W

Figure 5.1 is a cross section TEM image of the LMO thin films deposited on Si substrates at 700°C using a power of 50 W showing that the LMO thin film was successfully grown on the Si substrate using magnetron sputtering. The LMO film is about 80 nm thick and has a uniform structure and a very flat surface and a sharp interface with respect to the substrate. Between the film and the substrate, a bright interface layer with a thickness of about 4 nm was formed.

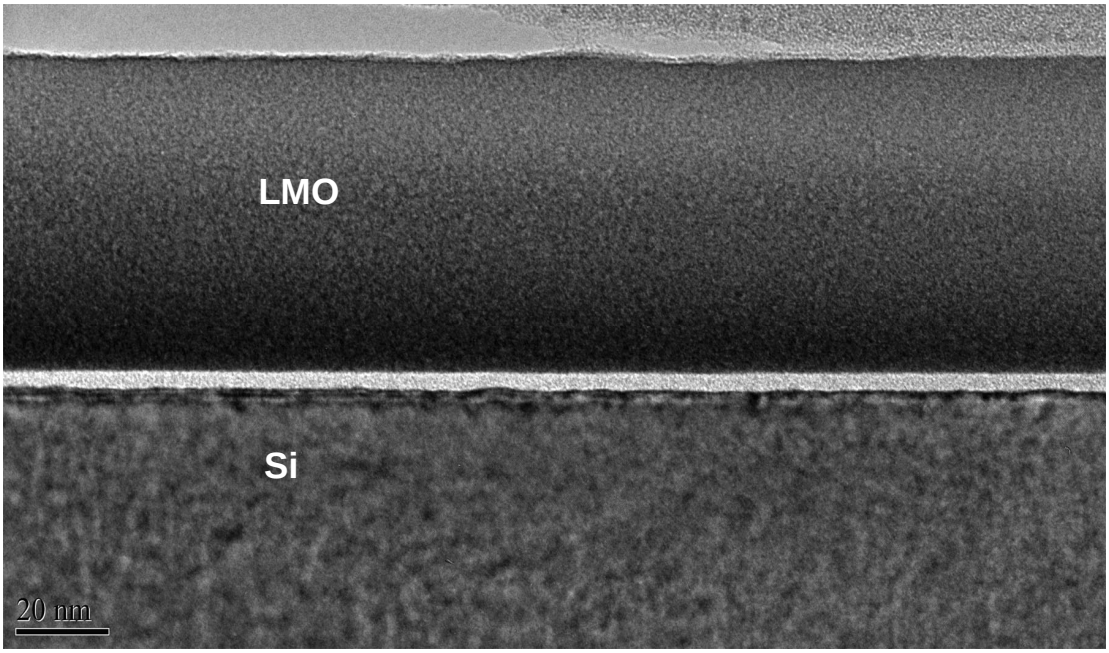

Figure 5.1 Cross-section HRTEM of LMO/Si at 700 °C using 50 W

Figure 5.2 is a SAED pattern taken from both t Si substrate and LMO film. It shows a single crystal diffraction pattern of Si and a diffuse ring pattern indicating that LMO film is an amorphous structure.

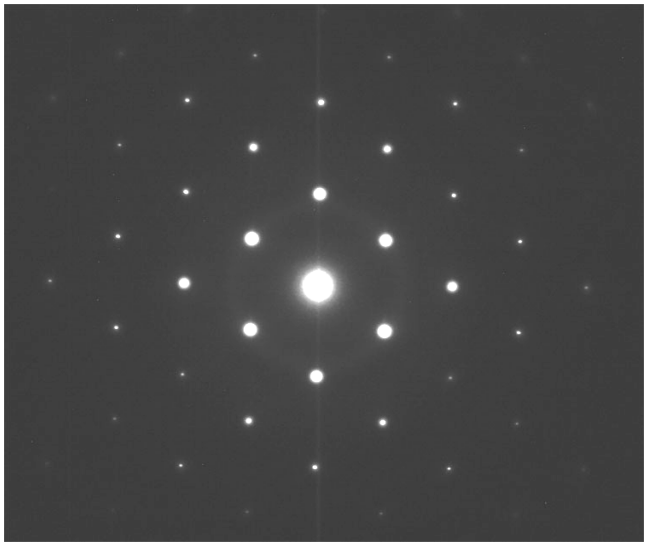

Figure 5.2 SAED pattern of LMO film and Si substrate deposited at 700 °C using 50 W

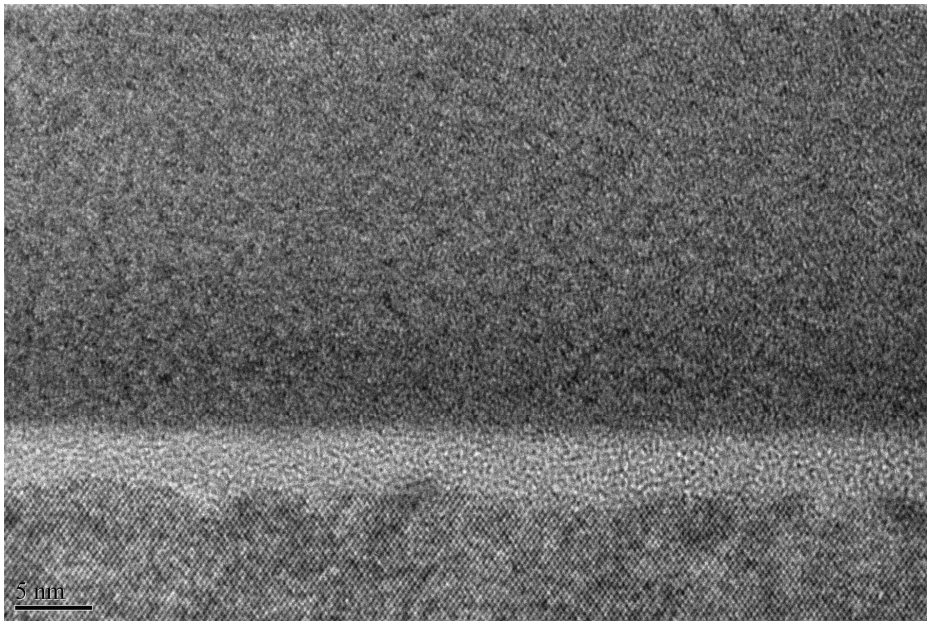

Figure 5.3 HRTEM image of LMO/Si interface for films deposited at 700 °C, 50 W

Figure 5.3 is a HRTEM image of cross-section LMO/Si showing that the overall film is amorphous structure because there are no any lattice fringes within the film.

5.1.2 LMO Thin Film on the Si Substrate Deposited at 700 ℃ 80 W.

Figure 5.4 shows the XRD result of the LMO thin film on the Si substrate deposited at 700°C and 80 W. No strong reflection of the LMO film and only a very weak peak located at a $2\theta = 33^0$ was observed. His indicates that the LMO film does not possess a good crystalline structure. It

possibly has some small gains with short range ordering formed in the film.

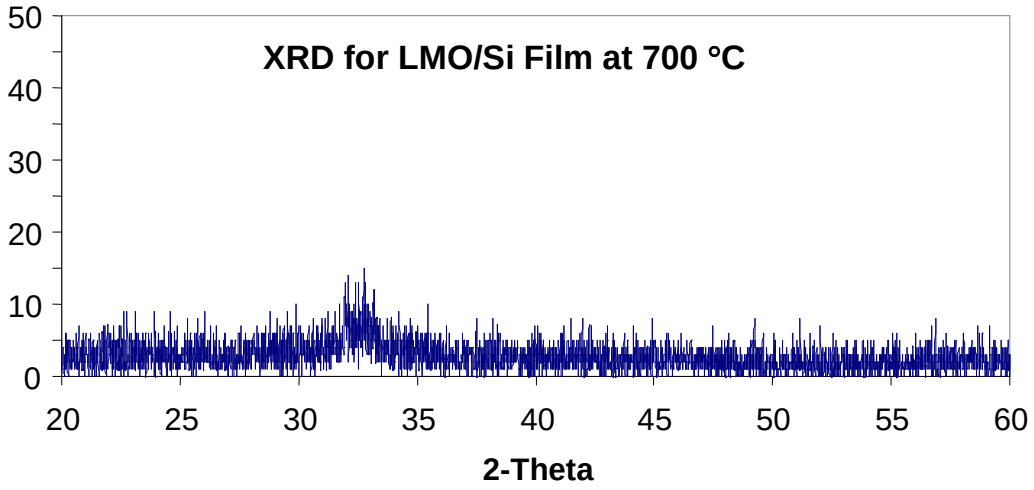

Figure 5.4 XRD of LMO film on Si deposited at 700 °C, 80 W

Figure 5.5 is a cross section TEM image of the LMO film deposited on Si at 700 °C, 80 W showing that the interface between the film and the substrate is flat and smooth. Thickness of film is about 60 nm. The film doesn't show a homogenous structure and can be divided into two regions (upper layer and lower layer). The lower layer that is close to substrate shows an amorphous structure with a thickness of about 10 to 15 nm. The upper regions have some variation of contrast which results from the crystalline particles formed in the area. The boundaries between the upper crystal area and lower amorphous area are clearly seen.

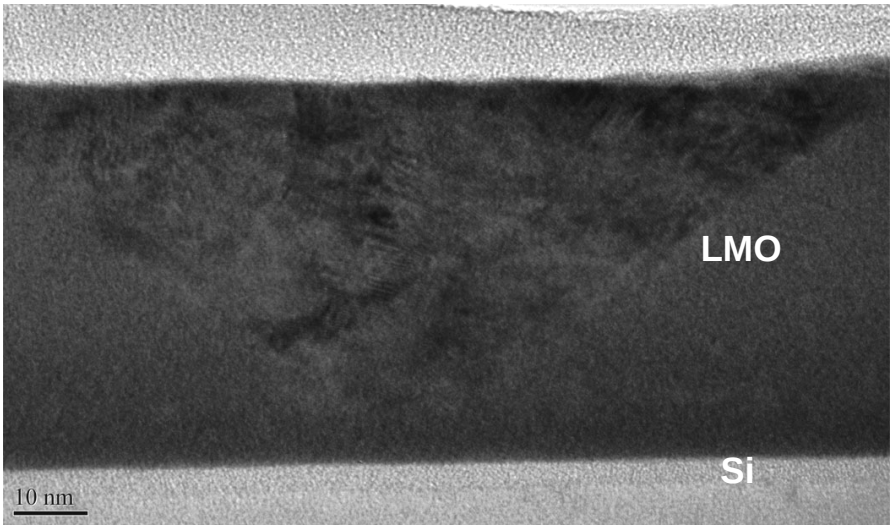

Figure 5.5 XTEM image of LMO/Si deposited at 700 °C, 80 W

Figure 5.6 is a SAED pattern taken from the film and the Si substrate. It shows the diffraction pattern of Si [110] zone axis and several weak rings corresponding to the reflection from the LMO film. This result presents the film as an nanocrystalline structure which is consistent with the XRD pattern that LMO film grown 700 °C, 80 W.

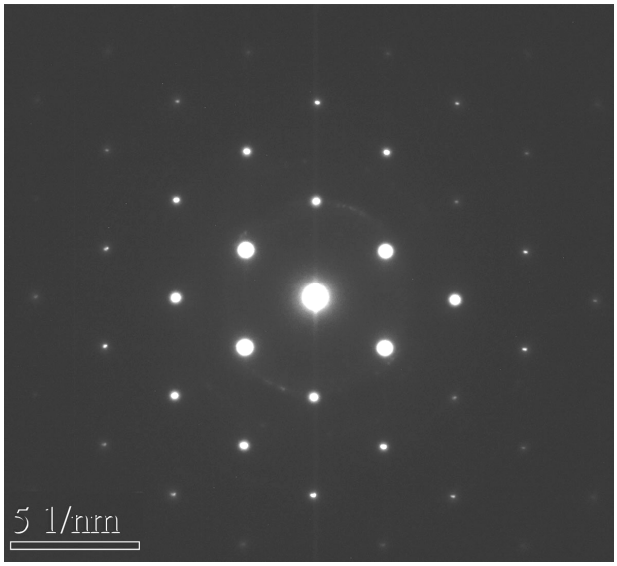

Figure 5.6 SAED pattern of the LMO film and Si deposited at 700 °C, 80 W

Figure 5.7 is a cross-section HRTEM image of the LMO/Si interface showing that there are some crystalline particles exhibited within the amorphous layer. In the lower area of the film, there is no lattice fringe and no contrast, all of the structure is uniform and smooth but in the crystal area, variation of contrast and the lattice fringe in the upper area demonstrate that some crystalline particles have grown in this area. Lattice fringes shows that the orientation of those particles is random and size of grains is about 15 nm and number of crystalline grain is rare and only some small areas produce this kind of crystalline grain.

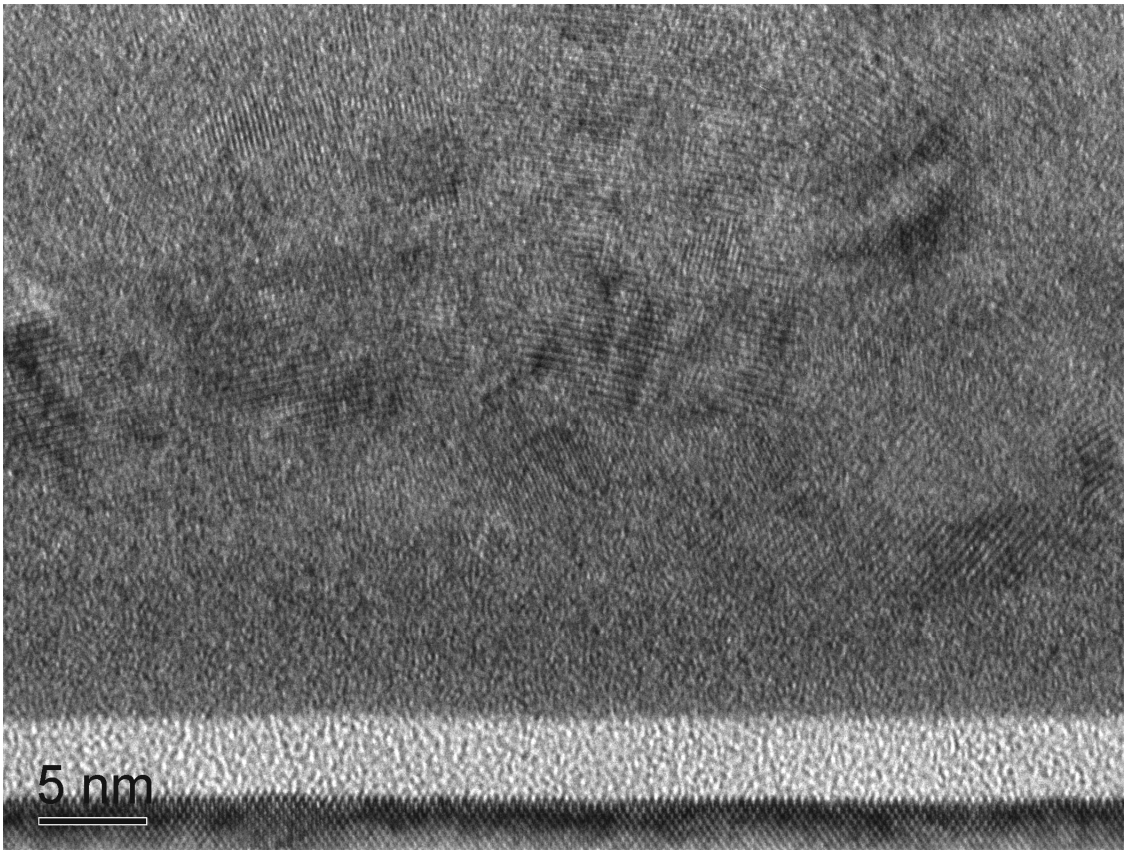

Figure 5.7 Cross-section HRTEM image LMO/Si interface deposited at 700 °C 80 W

Figure.5.8 is an HRTEM image taken from the upper area of the LMO film and this provides more information that there is some small crystal grains produced in this area. Lattice fringe is random and provide the evidence that particles are polycrystalline in structure.

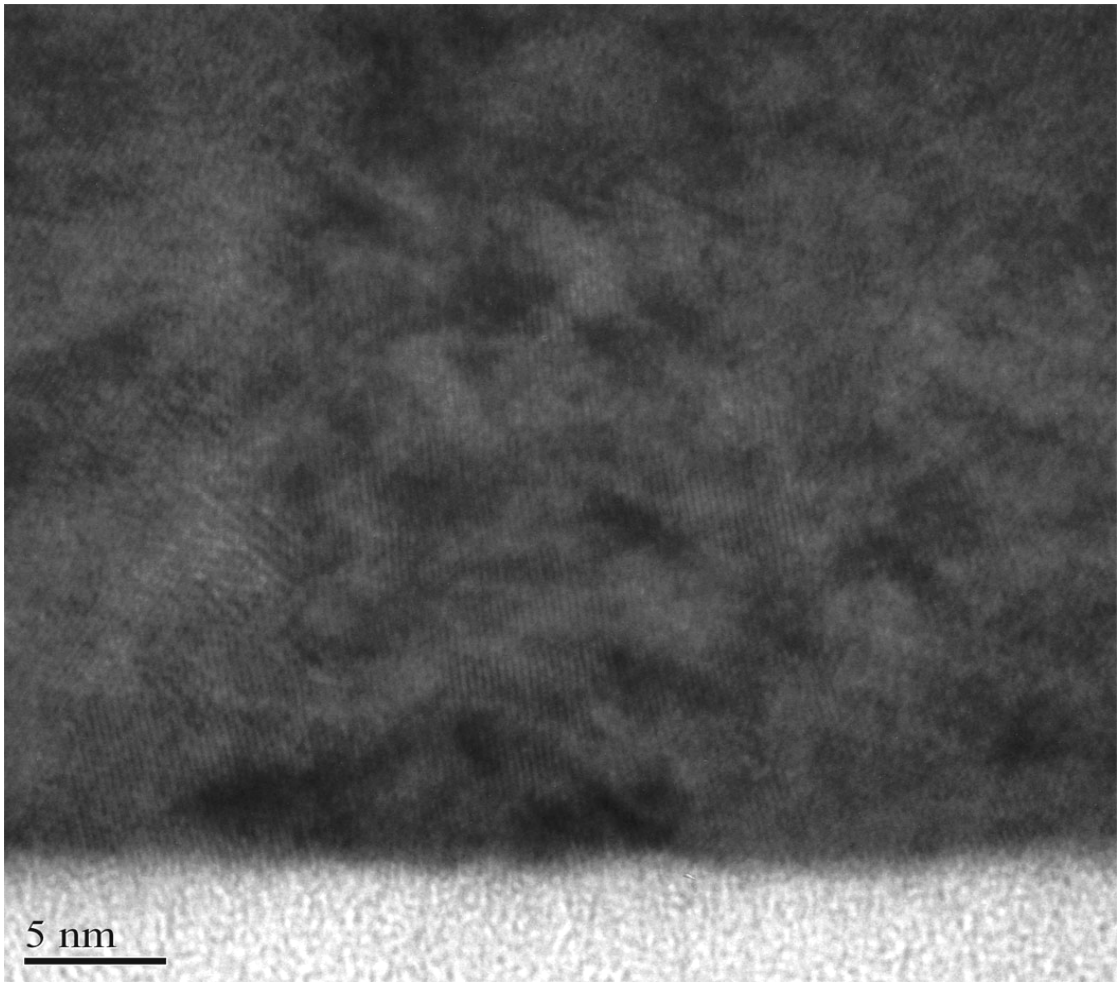

Figure 5.8 HRTEM image of the upper layer of the LMO film on Si deposited at 700 °C 80 W

5.1.3 LMO Thin Film on the Si Deposited at 750 ℃.

Figure 5.9 is a XRD pattern of the LMO thin film on the Si substrate deposited at 750 °C. There are four peaks in the diffraction diagram, the fourth peak is from the Si substrate and the other three small peaks are reflected from the LMO (100), (110) and (200) planes. In the terms of this XRD diffraction pattern, it is clear that crystalline LMO film has been successfully fabricated and is polycrystalline in structure. But whether it will have the expected self organized nano column structure and more details need to be investigated further by TEM.

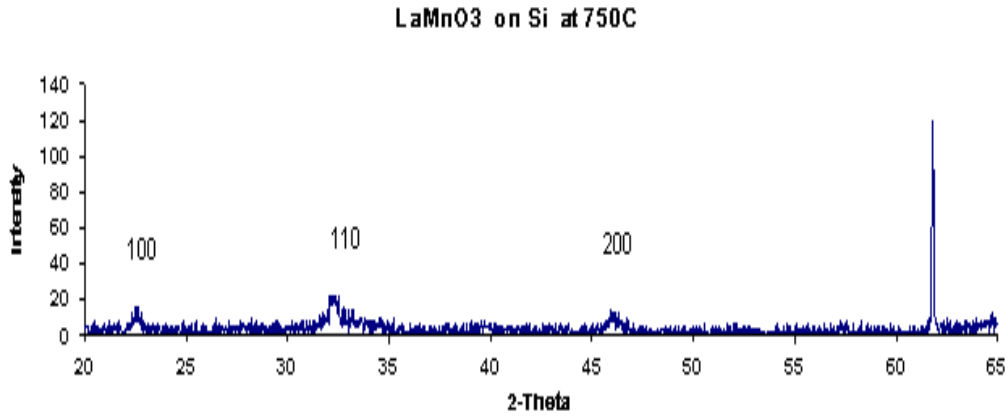

Figure 5.9 XRD of the LMO film on Si deposited at 750°C

Cross section and plan-view TEM observations are used to obtain 3-dimensional microstructure information of the thin films. Fig. 5.10 is a cross-section TEM image of the LMO on Si deposited at 750 °C. The LMO film has a flat surface, sharp interface and uniform thickness of about 60nm. Crystalline columnar structure can be seen across the film. The width the columnar grain range from 10 nm to 30 nm and the boundary of the column is well defined. The brighter layer at the interface between the film and substrate corresponding a SiO_2 layer of about 2 nm in thicknesses which can serve as a buffer layer to prevent the thin film and substrate atom from penetrating each other and benefit the stability of the thin film properties and structure. Based on the cross section TEM observation, it is certain that self -organized nano column crystalline LMO films have been successfully fabricated on the Si using magnetron plasma assisted sputtering.

Figure 5.10 is plane view bright field TEM image of the LMO film on Si deposited at 750°C showing distribution and morphology of columnar structures which consist of dark round shaped nano scale area and bright area. Dark round grains correspond to nano column grains with crystalline structure which reflect more electron beam demonstrating dark in BF image. Most of nano scale grains size varies from 10 nm to 30 nm which is in good agreement with observation of the cross section TEM. Some gains merge together to form relatively big gains.

SAED pattern of the LMO film at 750 °C exhibits sharp diffraction rings. By analysis of the diffraction pattern, it is known that the LMO film is polycrystalline with orthorhombic structure.

With respect to ring pattern, second ring is from the orientation (110) plane with stronger brightness which indicates that the LMO film is a slightly preferable textured film which is agreement with the XRD diffraction result.

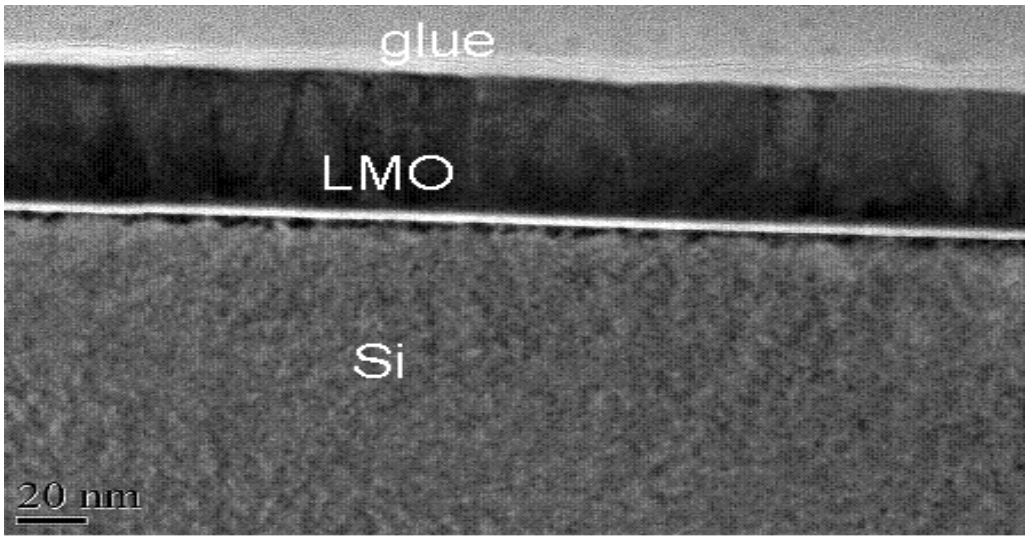

Figure 5.10 Cross-section TEM image of LMO/Si deposited at 750 °C

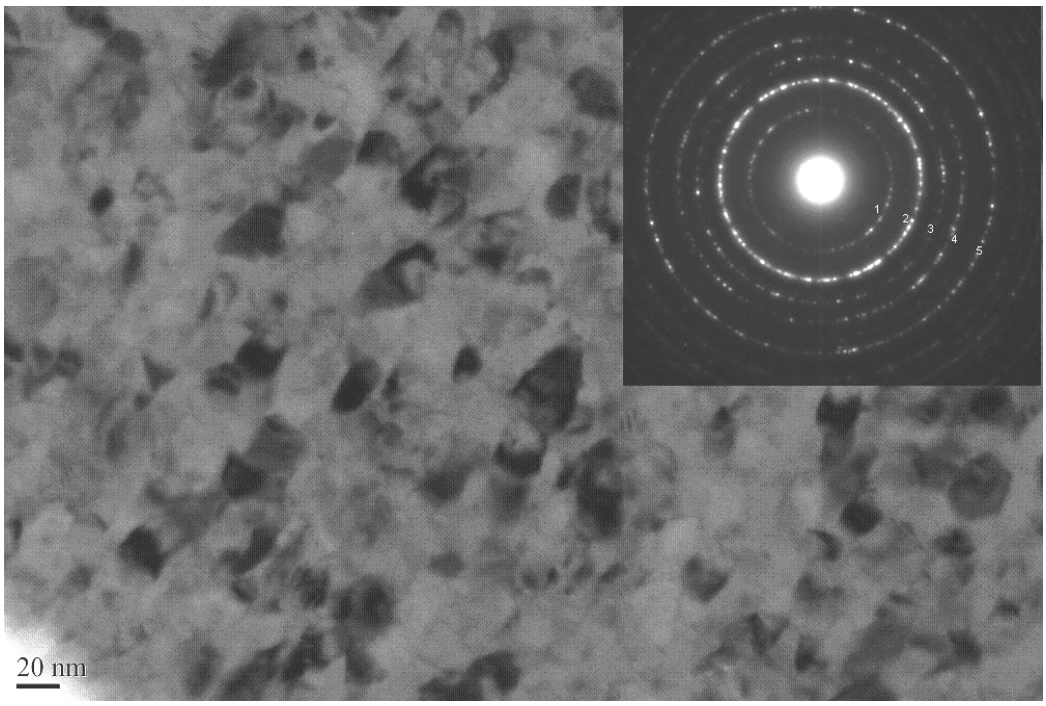

Figure 5.11 Plane view TEM Image of LMO film deposited at 750°C and the corresponding SAED pattern (inset)

For the nano column crystalline structure film, grain boundaries, interface between substrate and films and surface play important role in the properties of the thin film. HRTEM is an effective method to investigate the interface and grain boundary structure. Figure.5.12 is a cross-section HRTEM image of an as-deposited film which shows the microstructure of the film and interface between the substrate and film. The film was divided into two different layers (upper and lower part of thin film). The lower layer has an amorphous structure with no lattice fringes observed. The upper layer is composed of nano column crystalline structures with well defined grain boundaries and lattice fringe within the grains. Between the substrate and films, the white layer of an amorphous structure corresponds to SiO_2. This phenomenon shows that the LMO crystalline structure can grow from amorphous structure that LMO is lately self organized to form crystalline structure.

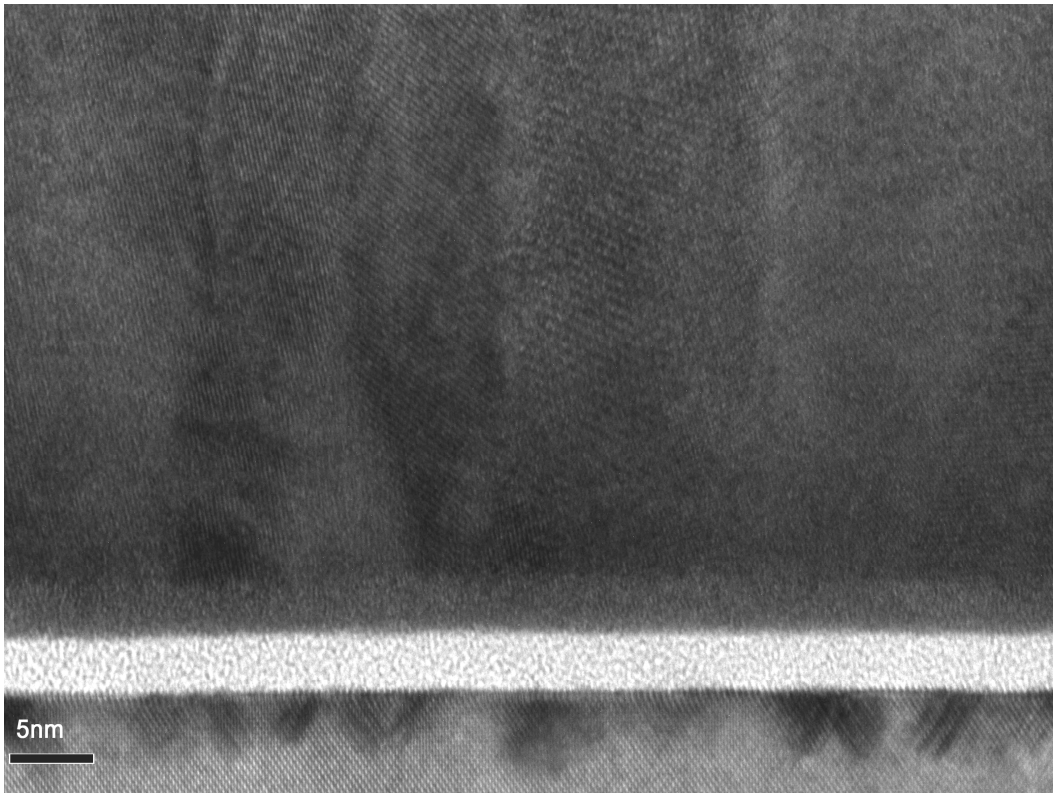

Figure 5.12 XHRTEM image LMO/Si deposited at 750 °C

It is clear that the width of nano columns arranges from about 15 nm to 25 nm. Lattice fringe in the nano pillars have been seen which provide further evidence of crystalline structure of the nano pillars. The lattice fringes in Figure 5.11 are randomly oriented indicating that the crystalline grains of the nano columns in the film are randomly oriented. This agrees with the XRD and SAED results.

Figure.13 is an HRTEM image of a plane view TEM foil of a LMO film showing the cross section of a single nano column and the boundary structure between the columns. In the single column, it is very clear that the lattice fringe arrange orderly and well-defined. This indicates that nano columns have good crystalline structure.

Investigation of the LMO films deposited at 750°C showed a different microstructure from those deposited at 700°C.

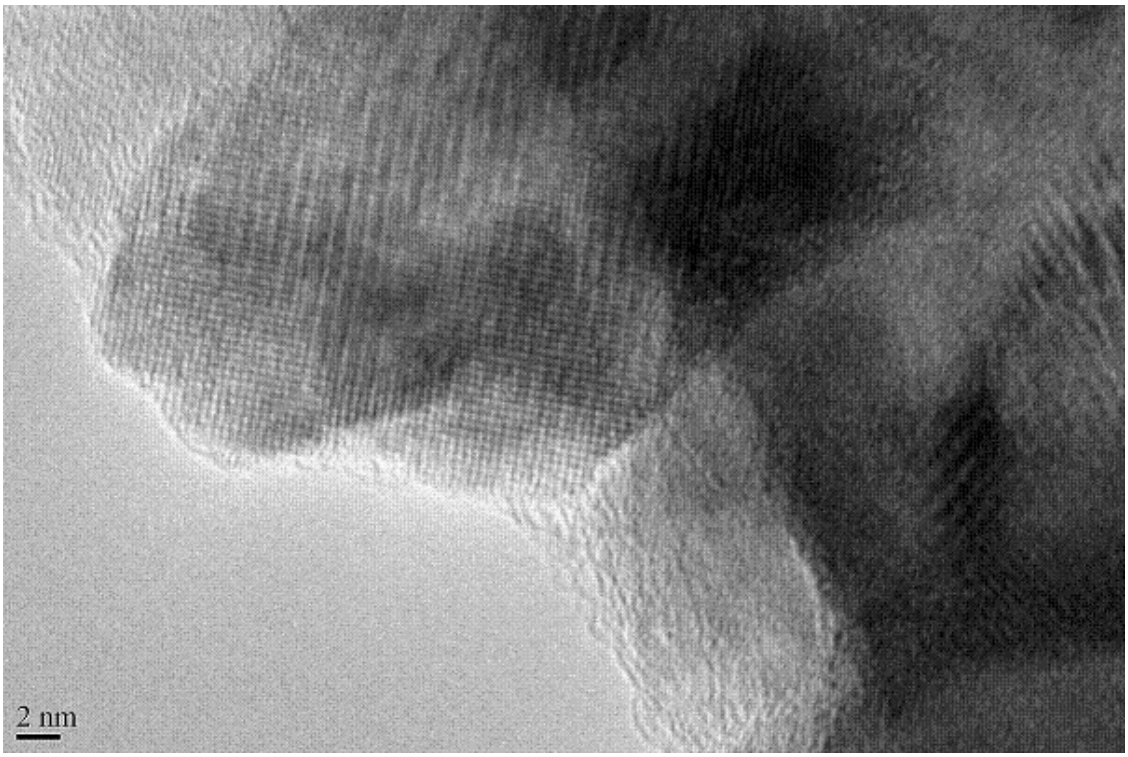

Figure 5.13 HRTEM image of a plan view LMO film on the Si deposited at 750°C

Summary of LMO Films on Si Substrate:

The LMO thin films were successfully fabricated on the Si substrates with a good interface and strong adhesion between the LMO films and Si substrates.

The microstructure of LMO films on Si substrate is dependent on the substrate temperature upon deposition. Deposited at 700°C, the film microstructure is mainly amorphous and exhibits only small areas with crystalline structure. Deposited at 750°C, LMO thin film is polycrystalline in structure with two layers (upper and lower); the lower layer is an amorphous structure and the upper layer is nano column crystalline structure. Therefore, the substrate temperature is a main influential factor of the quality of the LMO films and 750°C is the optimal deposition temperature. Deposition power also affects the quality of films but it has a smaller effect than the deposition temperature. Based on the thermodynamic theory, cooling rate is important factor that affects the form of the crystalline process; at low temperature, the formation of solidification is too fast, and the compounds do not have enough time to crystal before solidification completes. Therefore, at low temperature, fast rate of solidification led to form solid solution with amorphous structure. The elevated temperature, which reduces the rate of solidification, allows the compound to have sufficient time to form crystals.

The polycrystalline LMO films with nano column structure form because of strong tensile strain effects arising from the great misfit of about 28%.

Table 5.1 Misfit between the films and substrates

Misfit	LSMO (a_0 =0. 3889 nm)	LMO (a_0= 0.391 nm)
Si (a_0=0.5431 nm)	-0.2839	-0.2800
MgO (a_0=0.421 nm)	-0.076	-0.0712
LAO (a_0 =0.379 Å nm)	0.0261	0.0317

5.2 Epitaxial LMO Thin Films on(100) MgO substrate

LMO films were deposited on a single crystal MgO substrate using magnetron sputtering at 750°C, 30 W and 10 mTor. The misfit between LMO and MgO is -7.12%.

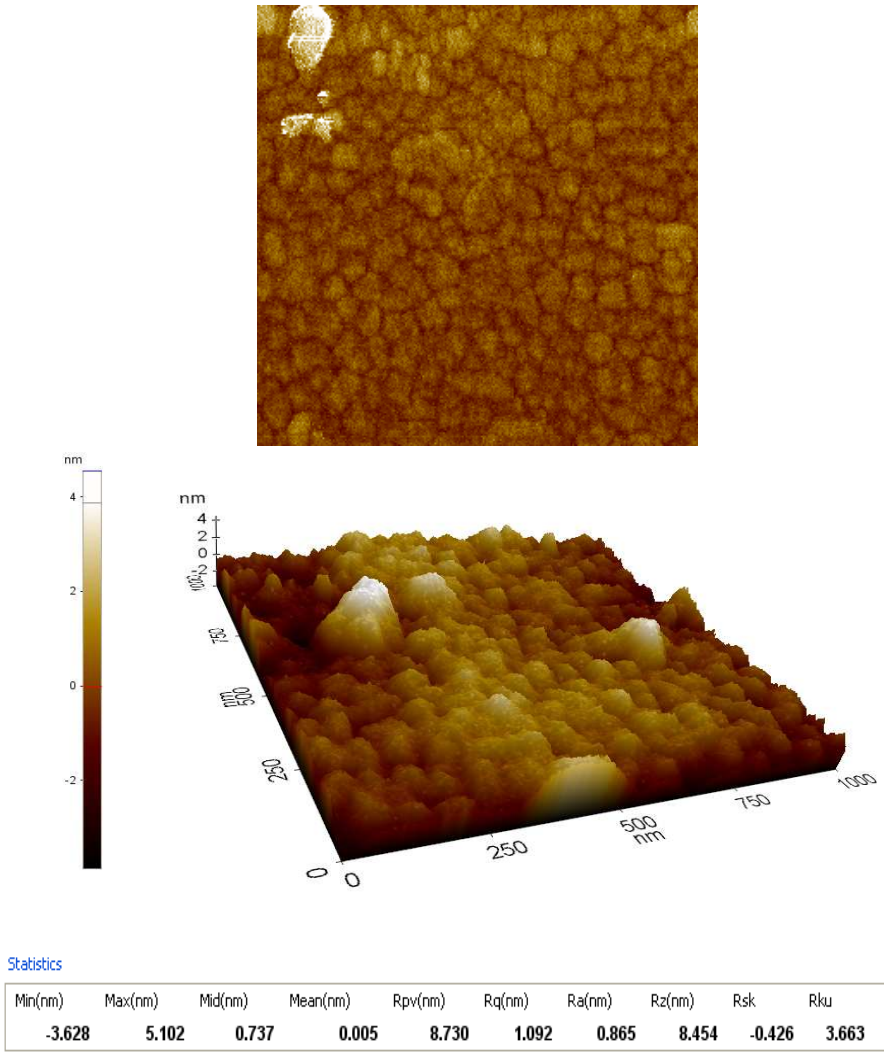

Figure 5.14 NCM AFM 2D, 3D image of LMO/MgO

5.2.1 Surface Properties by AFM

Figure 5.14 is a non-contact mode (NCM) AFM image showing 3D morphology of the surface of the LMO films grown on the MgO substrate. The surface of the LMO films is smooth and flat

with a mean roughness of about 0.005 nm. This film is uniform on the surface. No defects and cracks were found.

5.2.2 X-RAY Diffraction

Figure 5.15 is an X- ray diffraction pattern showing that there are three diffraction peaks. The highest peak is the reflection of the MgO (002) with spacing of about 2.1045 Å, and the other two peaks are reflections from the LMO thin film which could be identified as the LMO (001) plane with a spacing of about 3.915 Å and (002) with a spacing about 1.958 Å. With respect to this XRD diffraction pattern, it is clear that the film is an epitaxial film with misfit of about -7.12%.

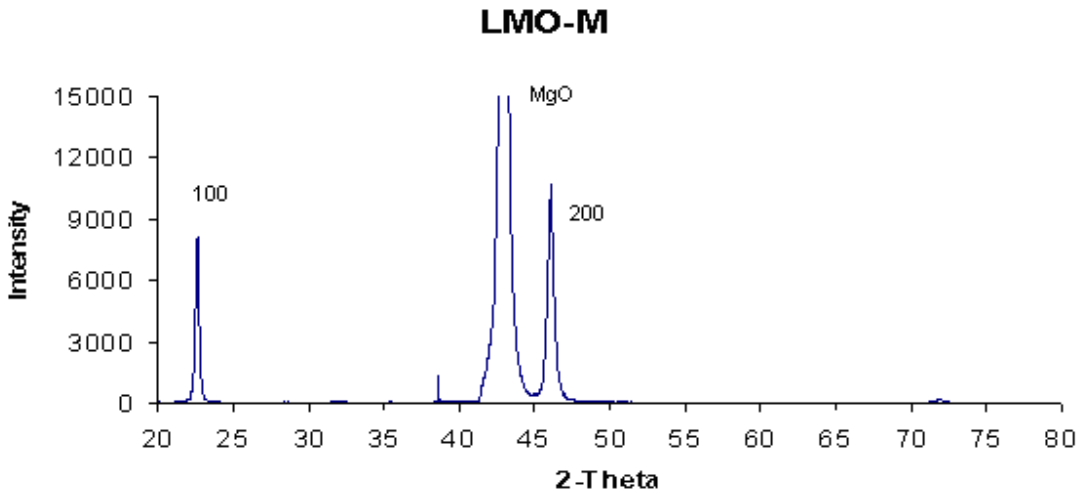

Figure 5.15 XRD of a LMO film on MgO deposited at 750 °C

5.2.3 TEM Analysis

Figure 5.16 is a bright field cross section TEM image showing that there are three layers. The bottom layer is the single crystal MgO substrate with a lattice constant 4.21 Å, the middle layer is the LMO film and the top layer is glue used to make cross section specimen. The films have definite interface between the film and substrate but interface is not flat and smooth. The reasons behind rough interface are still not known. The film thickness is about 60 nm and nano column structure with width ranging from 30 to 50nm across the whole thin film can be clearly

observed in the film. The grain boundaries of LMO were observed clearly and were almost perpendicular to the surface of the interface.

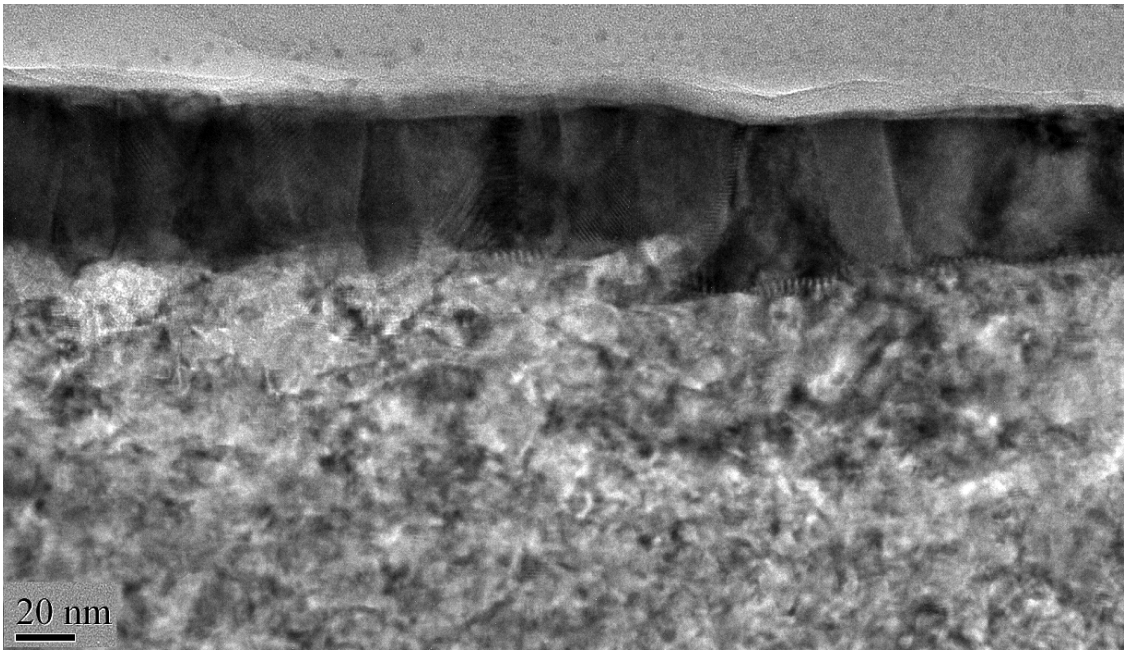

Figure 5.16 TEM image of LMO on MgO deposited at 750 °C, 30 W

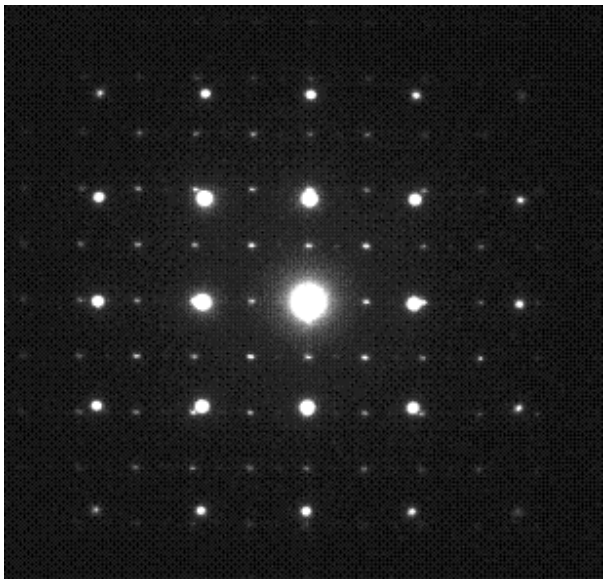

Figure 5.17 [100] zone SAED pattern of LMO film on MgO deposited at 750 °C

Figure5.17 is a SAED pattern taken from an covering both substrate and film which reveals the orientation relationship with respect to the substrate. The bright spots are considered as the diffraction pattern from single crystal MgO substrate along the [100] zone axis, the small spots are reflections from the LMO film. Figure 5.16 shows a superposition of two single crystal diffraction patterns from the MgO substrate and LMO film. It shows that the LMO film is an epitaxial film, which is also a single crystal and orientation relationship is $(001)_{LMO}//(001)_{MgO}$, $<100>_{LMO}//<100>_{MgO}$ (cubic setting). Misfit between the MgO substrate and the LMO film is about 7.13% measured from the SAED pattern. It can be obtained from the diffraction pattern that LMO film has an orthorhombic structure.

Figure 5.18 is an HRTEM image of the cross section LMO/MgO taken from a single column of the LMO which exhibits microstructure of a single grain with regular lattice fringe and boundary of grains. It was clearly demonstrated that the boundary area is almost an amorphous structure. Perfect lattice fringe in the grains shows that column is good crystal structure which also provides further evidence to epitaxial nano column structure of films. Films magnetic and electric properties are closely related to grain boundaries of nano columns. Dark contrast in the grain is defect field.

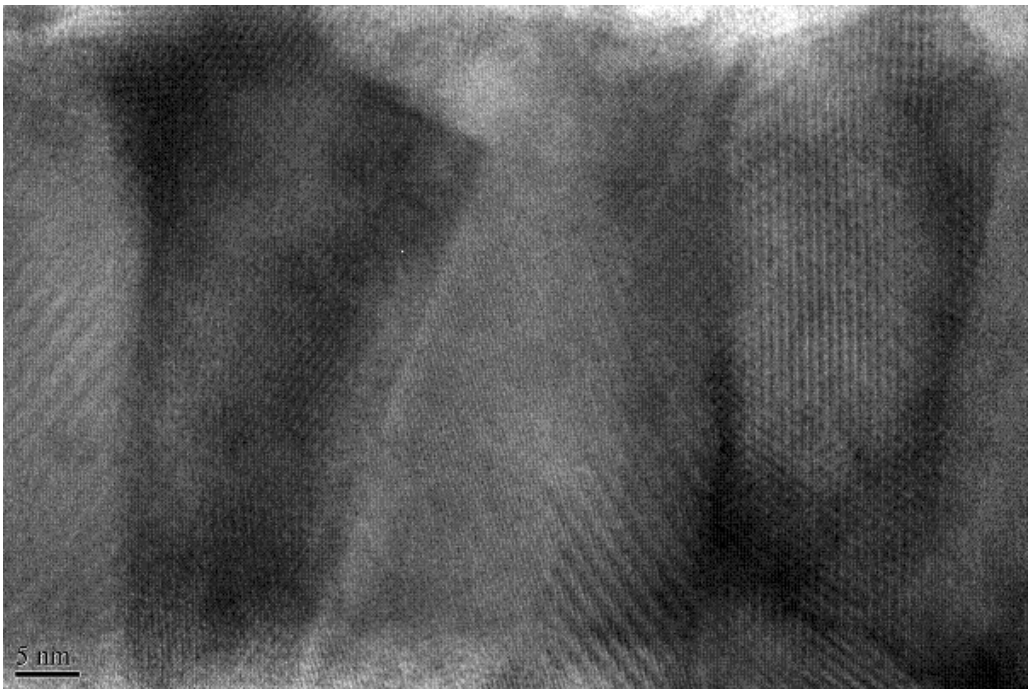

Figure 5.18 HRTEM image of a cross section LMO/ MgO deposited at 750 °C

Figure 5.19 is an HRTEM image of cross section TEM showing the structure of the interface between substrate and LMO film. The horizontal dark line in the middle of image is the interface. The upper layer is LMO film and lower layer is the MgO substrate. Observation of lattice fringe shows that it is epitaxial film grown on the substrate because both sides of interface are similar. Above SAED pattern also can testify that the film is an epitaxial single crystal structure.

TEM observation also shows periodical defects in the substrate adjacent to where there are large numbers of dark contrast in the substrate which is in agreement with the reports in the literature that substrates quality will play an important role in the film. Periodic defects can be seen along the areas adjacent to the surface of the substrate and also a small area that is totally amorphous structure. It demonstrates definite defects in the LMO film. The defects are in the positions where there are a large number strains.

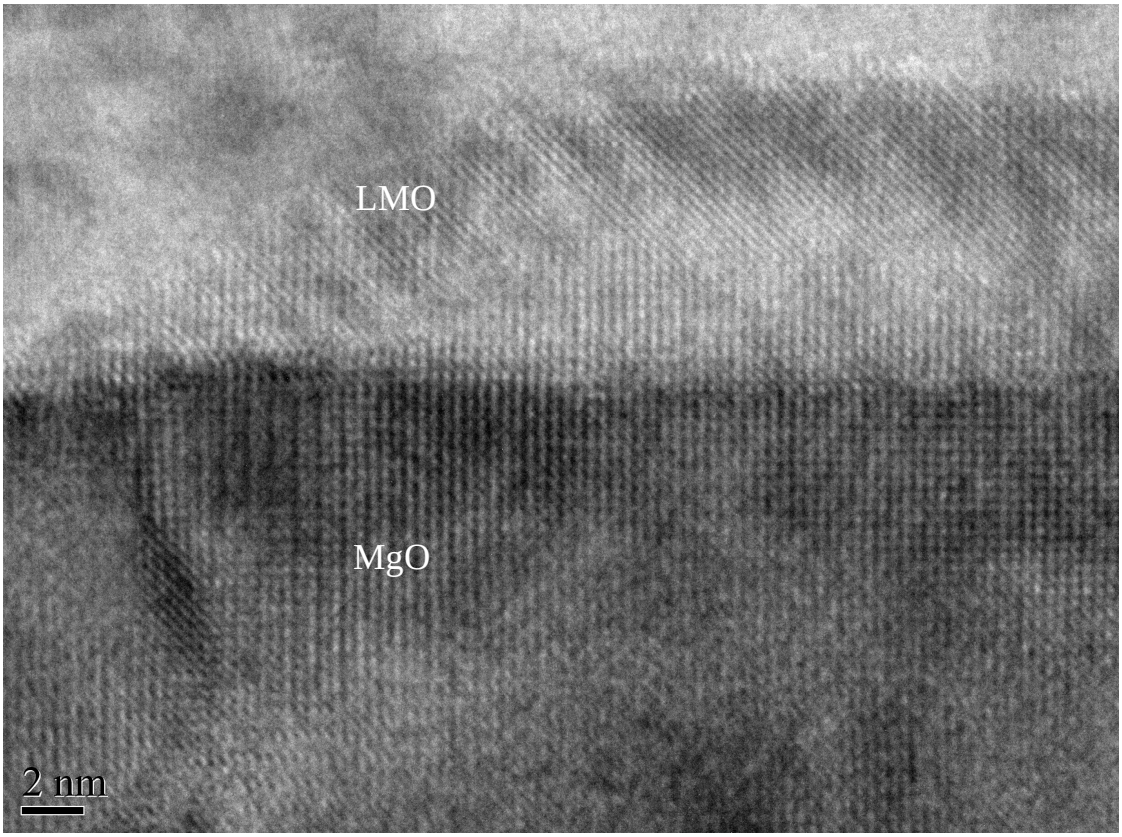

Figure 5.19 HRTEM image of cross section TEM of LMO/MgO deposited at 750 °C

5.3 Epitaxial LSMO Film on the MgO Substrates

LSMO thin films were deposited on a single crystal MgO substrate with lattice constant of about 4.21 Å at 750°C, 30 W and 10mTorr using RF sputtering.

5.3.1 Surface Properties by AFM

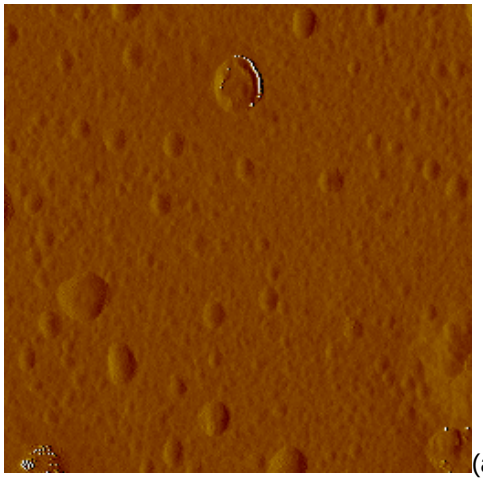

(a)

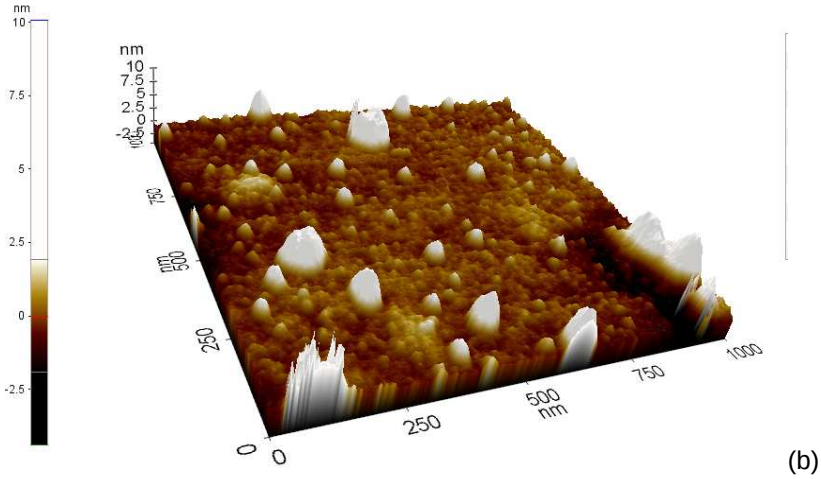

(b)

Statistics

Min(nm)	Max(nm)	Mid(nm)	Mean(nm)	Rpv(nm)	Rq(nm)	Ra(nm)	Rz(nm)	Rsk	Rku
-4.398	10.073	2.838	-0.004	14.471	1.039	0.595	13.451	-2.553	14.435

Figure 5.20 (a), (b) NCM AFM 2D, 3D image of LSMO/MgO

Figure 5.20 (a),(b) is an NCM AFM image showing the morphology of the LSMO films grown on MgO with a very smooth surface and a mean roughness is about of -0.004nm. Connected spherical particle arrays are very homogenous and smaller than the LMO films on the MgO. Based on the AFM results, the Sr-doped manganite films grown on the MgO posse better surface quality than pure manganite films.

5.3.2 XRD Analysis

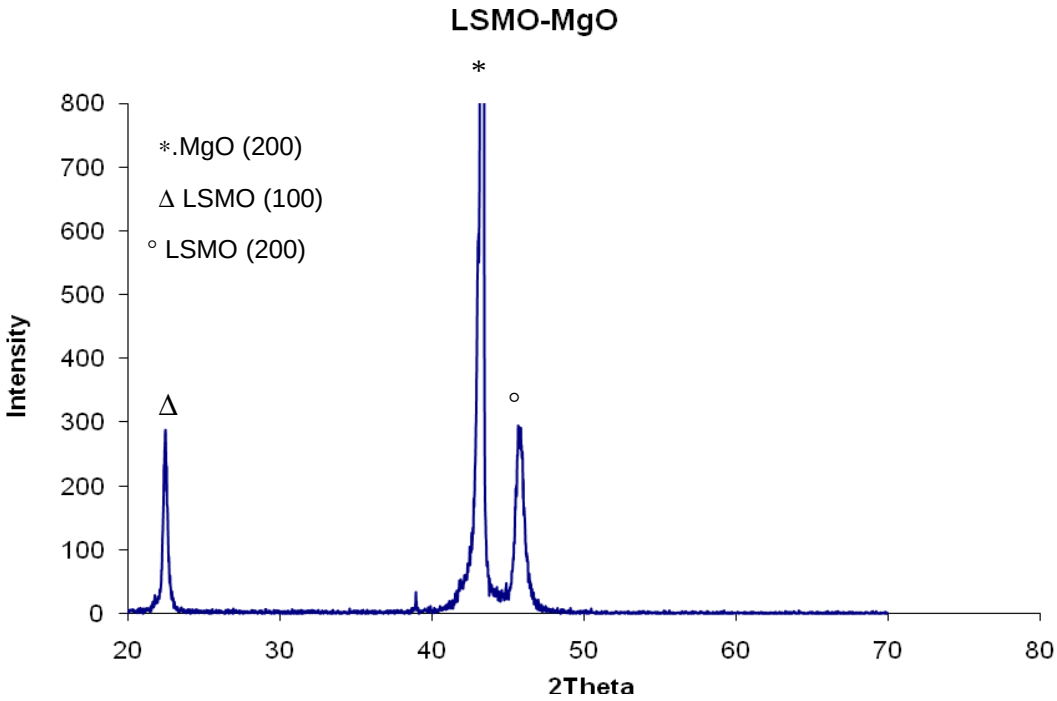

Figure 5.21 XRD of LSMO on MgO deposited at 750°C

Figure 5.21 is an XRD pattern of LSMO thin film on MgO showing that there are three peaks, the top sharp peak is from the MgO (200) with spacing 2.088 Å and the two small peaks are from LSMO (100) with a spacing of about 0.3910 nm and LSMO (200) reflection with spacing about 1.9830 Å. It is clear that the LSMO is an epitaxial film with good texture structure. In terms of this XRD pattern, the value of misfit can be estimated as -0.0762.

5.3.3 LSMO films Analysis by Low Magnification of TEM

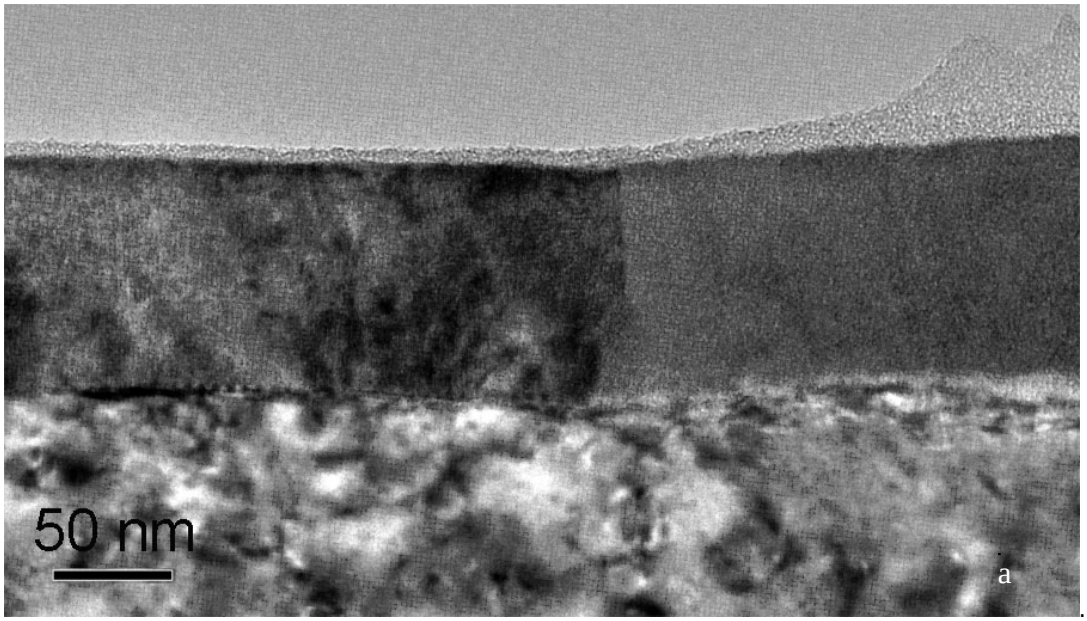

Figure5.22 TEM image of LSMO film on MgO substrates at 750°C

Figure 5.22 is an HRTEM image of cross section TEM at low magnification showing the interface between the substrate and film. From this it can be seen that LSMO film is clearly smooth the surface of the film is very flat and in the film there are two different domains. One domain shows the nano column structure with various grain sizes the other domain does not display any column structure. It is clear that the LSMO thin film has a crystalline structure. The thickness of the film is 70 nm.

Figure5.23 (a) is (001) zone axial SAED pattern taken from the interface of LSMO and MgO and (b) is (001) zone axial SAED pattern taken from the substrate MgO. These showed that LSMO films are an epitaxial single crystal structure grown on MgO substrate with the orientation $<100>_{LSMO}//<100>_{MgO}$. We also can determine that LSMO films are orthorhombic in structure with a two-type domain. Misfit of films is -0.0762.

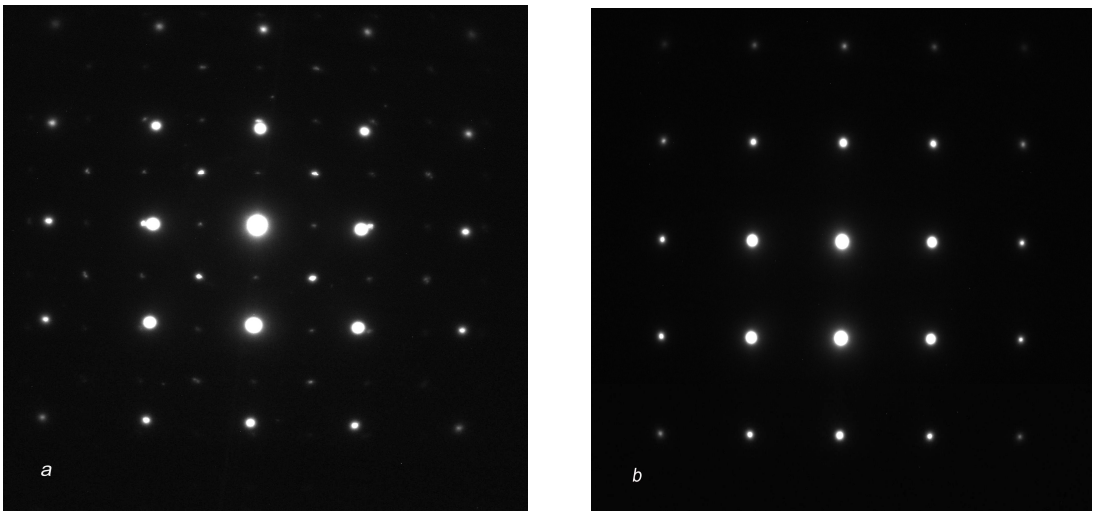

Figure 5.23 a, b [100] zone SAED taken from the interface and substrates, respectively of the XTEM of LSMO films on MgO

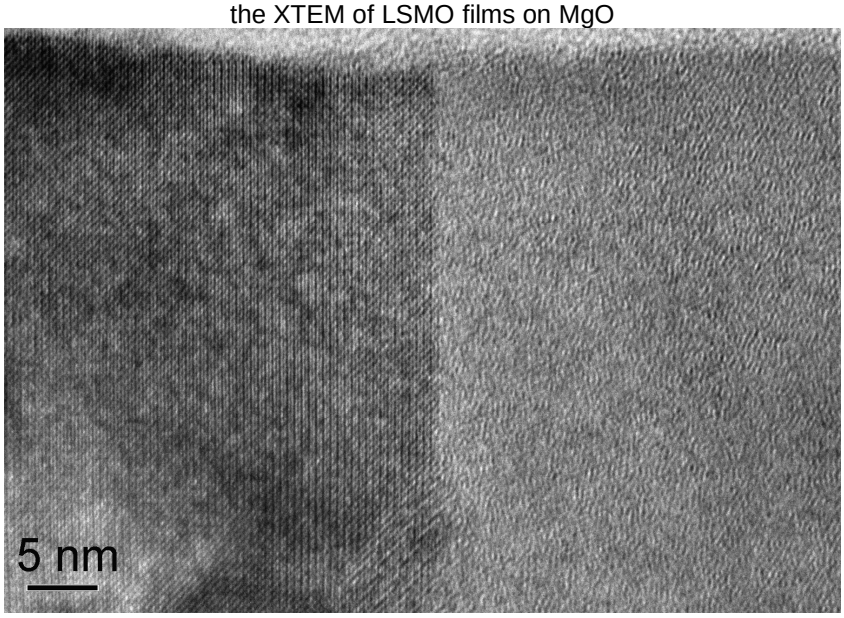

Figure 5.24 HRTEM image of LSMO film on MgO substrate at 750°C

Figure5.24 is an HRTEM image of LSMO films clearly showing the well-defined interface between two domains of LSMO films. On the left side of the interface, it is a crystalline structure with strong and ordered lattice fringe but on the right side domain no lattice fringe can be seen.

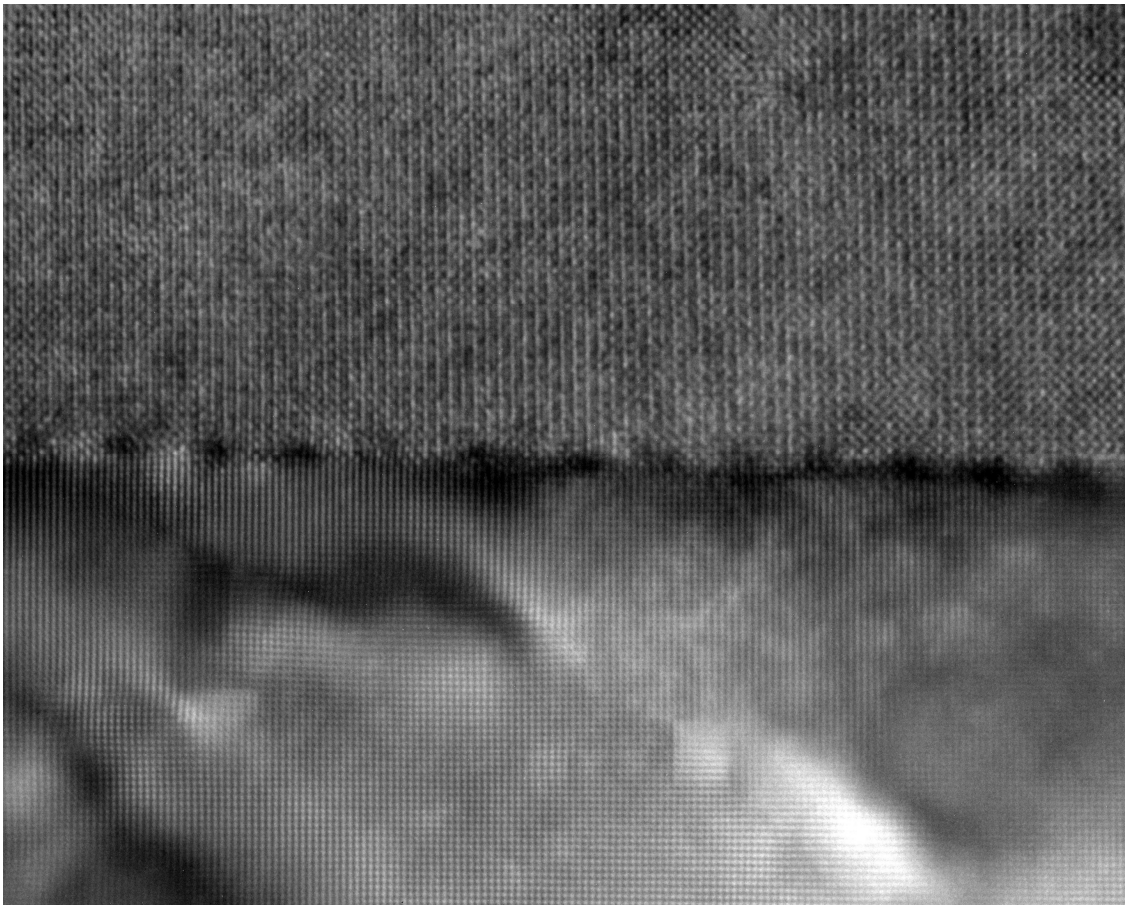

Figure 5.25 HRTEM image of the LSMO film on MgO at 750 °C

Figure 5.25 is an HRTEM image of cross section of LSMO on MgO revealing that the film of LSMO is an epitaxial single crystal structure and the lattice fringe of the LSMO film is uniform. There are some dark contrasts on the interface which are the edge dislocations. Based on the lattice fringe of the LSMO films, we also determine that the films are orthorhombic in structure.

The LSMO films present high quality crystalline thin films with uniform lattice fringe. It shows that the films are epitaxial films which agree with the XRD and SEDP results. Some dark contrasts at the interface between substrate and film are periodic edge dislocations which arise from the misfit of films and substrate.

Discussion:

Based on the above analysis, the epitaxial LSMO and LMO films were successfully fabricated by RF magnetron sputtering. LMO films have nano column structure with upright grain boundaries and LSMO films also have nano column structure. Compared with the polycrystalline LMO films grown on the Si substrate with a lattice misfit of 28%, LSMO and LMO films epitaxially grown on MgO with misfit of 7.62% and 7.13% respectively have better quality. It is clear that relative smaller misfit between the substrate and films will result in better films which agree with the result found in the literature. Substitution of La with the Sr reduces the lattice constant.

From the HRTEM image, periodic defects can be observed in the interface between the film and substrate which arises from the misfit of films (LMO, LSMO) and substrate (MgO).

5.4 LMO Thin Film on the LAO

LMO films were deposited on a single crystal of LAO (100) substrate at 750°C and 30 W to study the effect of substrate.

5.4.1 Surface Properties by AFM

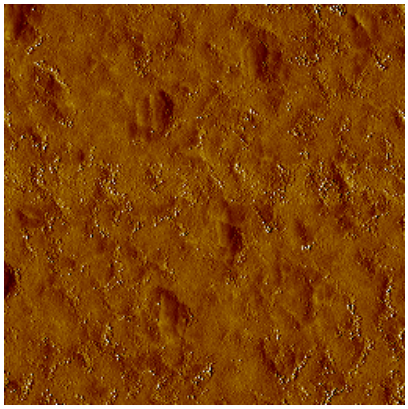

(a)

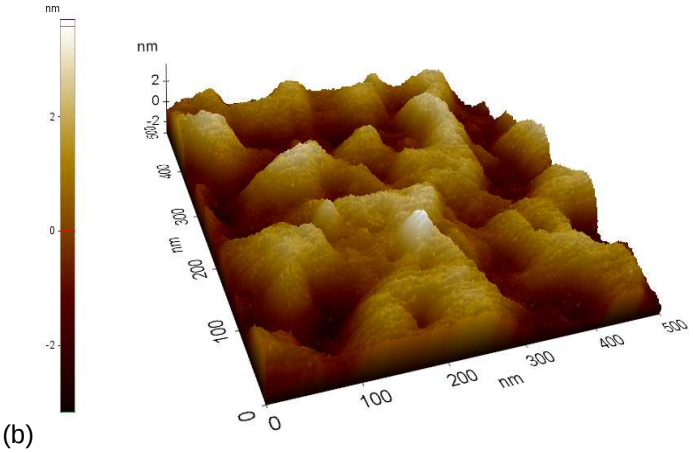

(b)

Statistics

Min(nm)	Max(nm)	Mid(nm)	Mean(nm)	Rpv(nm)	Rq(nm)	Ra(nm)	Rz(nm)	Rsk	Rku
-4.004	12.933	4.464	0.000	16.937	1.768	1.380	16.246	-0.959	4.780

Figure 5.26 (a), (b) AFM NCM 2D, 3D image of LMO/LAO films

5.4.2 XRD Analysis

Figure 5.27 shows an XRD pattern of LMO films on the LAO substrate. Five peaks are presented in the diffraction pattern diagram, two high peaks are from the LAO substrate reflection, and two lower peaks slightly shifted from the high peak are from the reflection of LMO. Based on the XRD pattern, we can know the films crystalline structure is good match the substrate crystal

structure. Because the substrate is a LAO single crystal, the film structure is similar to the substrate microstructure. The only difference from this XRD diffraction pattern is lattice spacing. The growth orientation of LMO between the films and substrate was determined as LMO (100) // LAO (100) Therefore, very good epitaxial LMO thin film was fabricated by the magnetron RF sputtering.

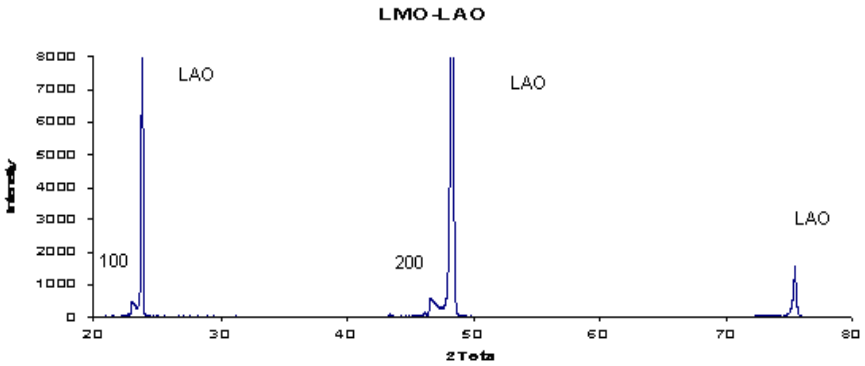

Figure 5.27 XRD of LMO film grown on LAO substrate deposited at 750°C and 30 W

5.4.3 Conventional TEM of LMO Films on LAO

Figure 5.28(a) is cross section TEM observation. The LMO films successfully deposited on the LAO substrate at 750°C and the surface of the film and the interface between the films and substrate were clear, smooth and flat. Compared with the LMO on the Si and MgO, no nano columnar structure can be observed. Figure5.28 (b) selected area diffraction pattern confirmed the LMO films were a single crystal structure and the misfit between the substrate and films is -0.2800, as for this direction, we can deduct that orientation relationship are <100>LMO//<100>LAO.

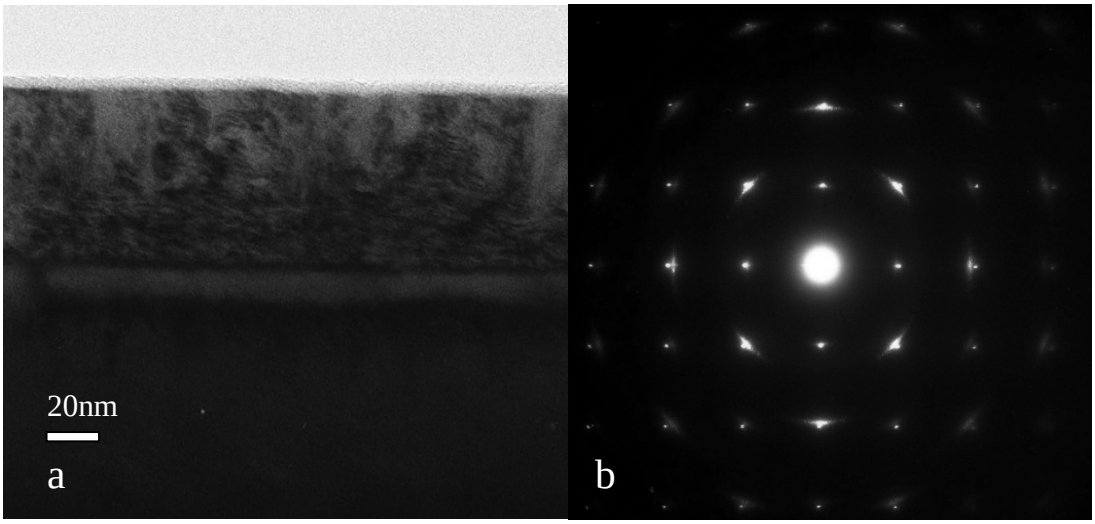

Figure 5.28 TEM image (a) and SAED pattern (b) taken from interface between the LMO/LAO cut from the direction 1

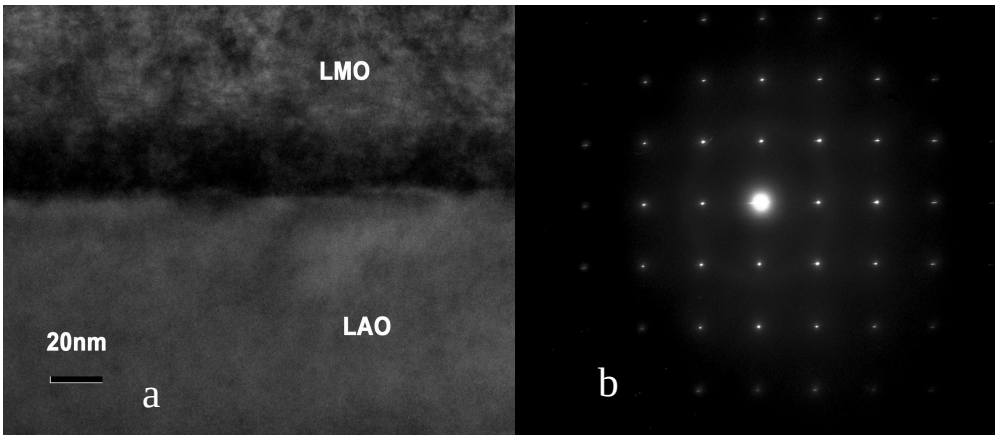

Figure 5.29 (a) cross section TEM observation of LMO/LAO and (b) [100] zone SAED pattern of interface from direction perpendicular to the direction 2

Figure 5.29 (a) is a low Magnification image of LMO thin films grown on the LAO substrate whose TEM observations are perpendicular to the direction 1. Observations of the TEM image indicated that the LMO film is about 70nm in thickness. The surface of the film is very flat and smooth and the interface between the substrate and films is very clear. We did not observe nano pillar structure in the films. SAED pattern taken from interface between the LMO and LAO showed that LMO films are an epitaxial single crystal structure with a lattice constant

a_0=0.391nm.Combining the direction 1 with direction 2 SAED pattern result, we can determine that the LMO films are cubic in structure.

5.4.4 Interface Study by HRTEM

Figure 5.30 is an HRTEM image of XTEM showing that LMO films epitaxially were grown on the LAO substrate. The lattice fringe on the LMO films continued to the lattice fringe of the substrates. At the area of interface some dark contrast separated the substrate and films, this dark contrast showed that some dislocations were presented at the interface. The lattice fringes in the films are uniform and this confirmed the LMO films are a single crystal structure.

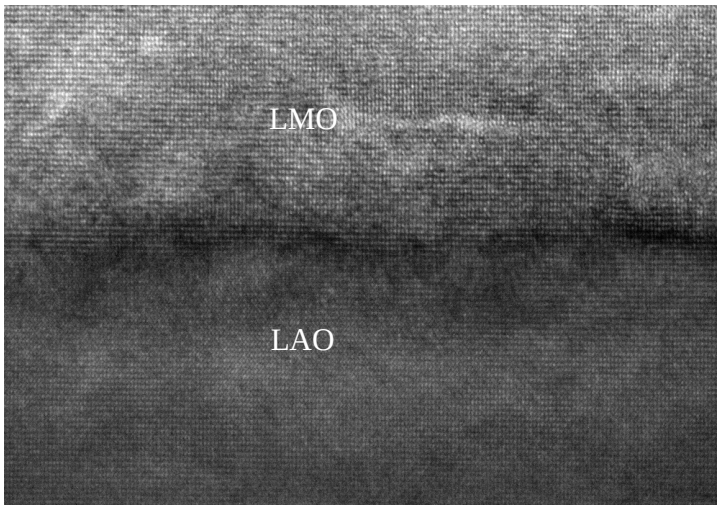

Figure 5.30 HRTEM image of cross section of LMO/LAO

5.5 LSMO Thin Film on LAO Substrate

5.5.1 AFM Analysis

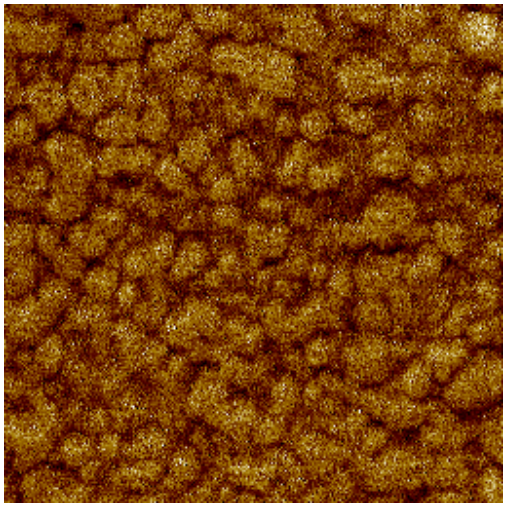

(a)

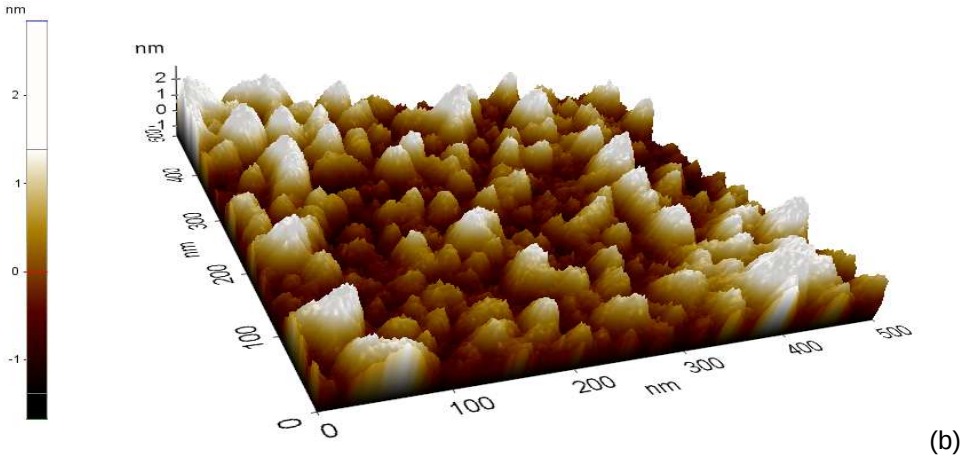

(b)

Statistics

Min(nm)	Max(nm)	Mid(nm)	Mean(nm)	Rpv(nm)	Rq(nm)	Ra(nm)	Rz(nm)	Rsk	Rku
-1.675	2.844	0.584	0.000	4.519	0.744	0.602	4.441	-0.663	3.074

Figure 5.31 (a) (b) AFM NCM 2D, 3D image of LSMO/LAO

5.5.2 XRD Analysis

The condition of LSMO grown on the LAO substrate at 750 °C,

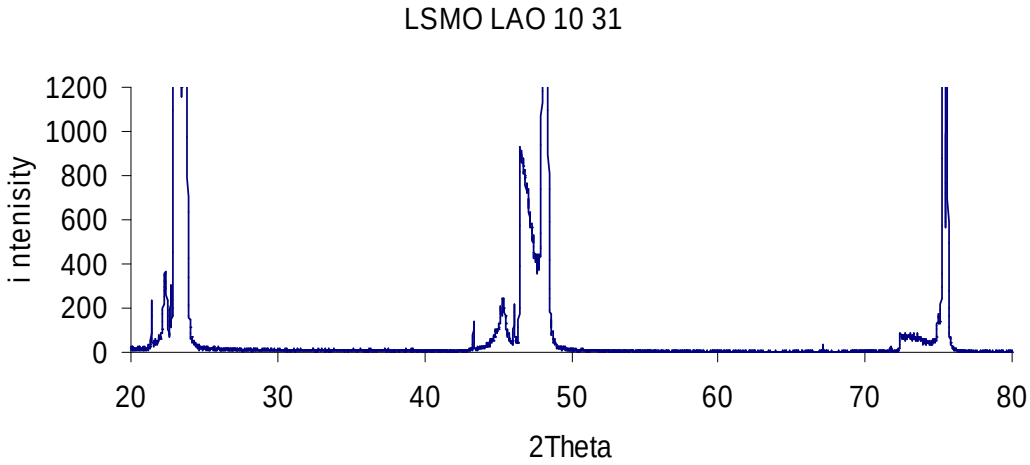

Figure 5.32 x- ray diffraction pattern of LSMO thin film on the LAO substrate

XRD analysis primarily demonstrates that LSMO on LAO is crystalline structure and it should be an epitaxial film.

5.5.3 TEM Analysis

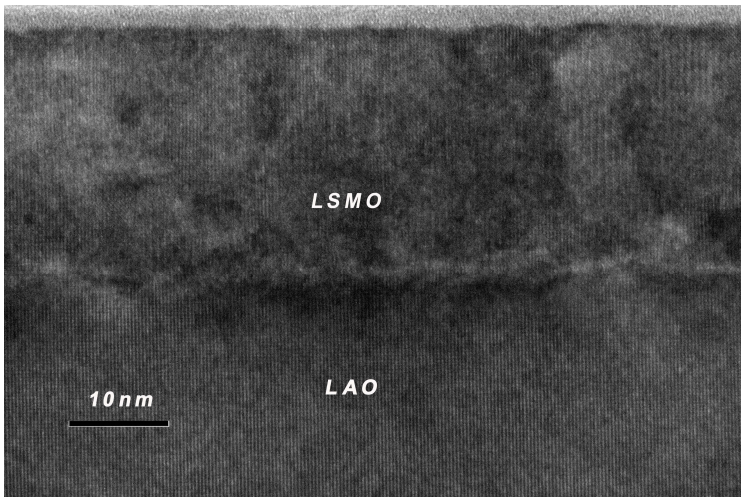

Figure 5.33, Cross section TEM image of LSMO film on LAO

Figure 5.33 is a cross section TEM image showing that the films were successfully grown on the single crystal LAO substrate. The thickness of LSMO films are about 26 nm. We also do not

find the nano columnar structure in the films Interface between LSMO and LAO can be clearly seen. Coherent lattice fringe can be observed at the interface which demonstrates that the LSMO were also a single crystal structure and all the films have uniform lattice fringe. It is clear that LSMO thin films were very good single crystal films.

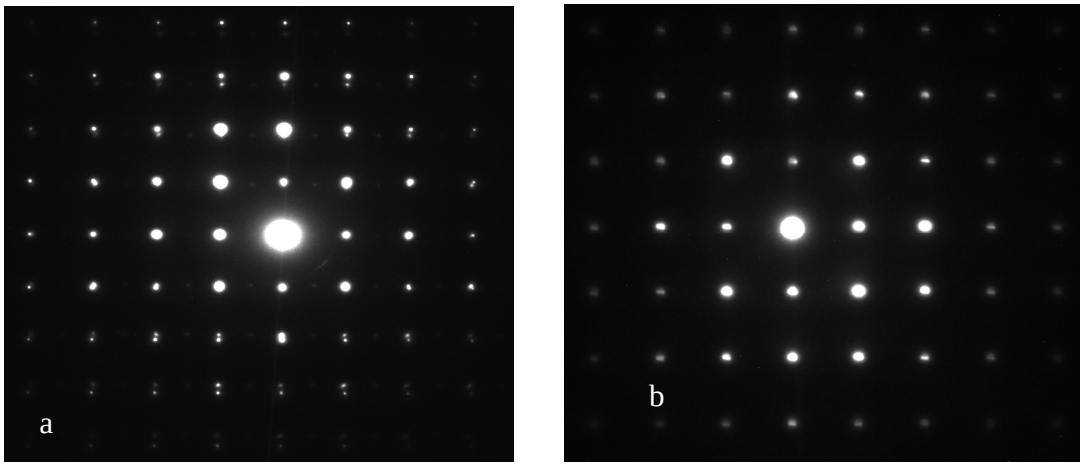

Figure 5.34 a SAED pattern taken from interface between LSMO and LAO, b, SAED pattern taken from substrate LAO at (100) zone axis

Figure 5.34 is (100) zone axial SAED pattern of the interface between the LSMO/LAO and b is the SAED pattern taken from substrate LAO. Compared with them, we can be easy to find the diffraction pattern of the films in the fig 36a. it can know that LSMO films are orthorhombic structure and are epitaxially deposited on the LAO with misfit about 3.15%, and orientations relationship between the films and substrate is <100>LMO//<100>LAO.

5.5.4 Interface analysis of LSMO films on LAO by HRTEM

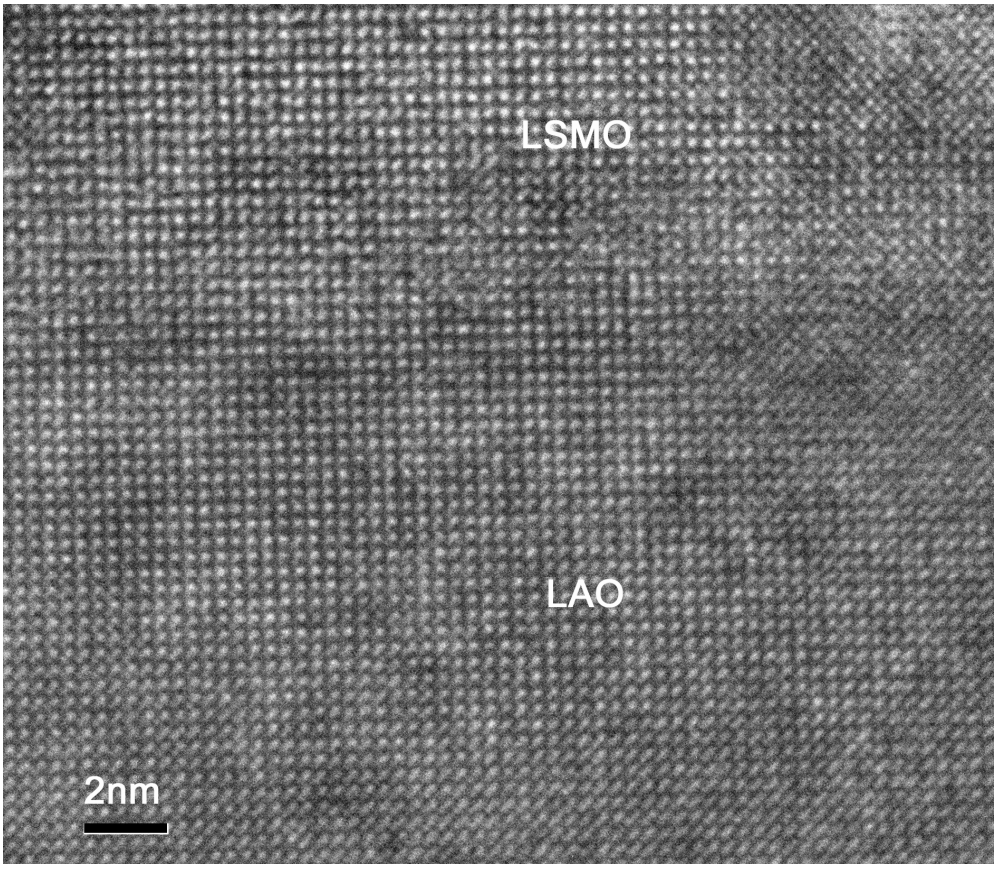

Figure.5.35 HRTEM image of cross section TEM of LSMO/LAO

Figure 5.35 is a HRTEM image showing the interface between LSMO films and substrates with homogenous lattice fringe in the films. The lattice fringe of the interface is clear and uniform and there is free-edge dislocation observation in the interface. The interface of LSMO and LAO is a perfect coherent structure. It is clear that the LSMO is a single crystal with an orthorhombic structure.

Discussion of LMO and LSMO Films Grown on LAO Substrate

Both LMO and LSMO thin films were an epitaxial single crystal grown on the single crystal LAO substrates.

From the TEM analysis, both films are a cubic structure. Compared with nano column LMO on the Si which grew from island nucleation, LMO and LSMO films grow in the layer type nucleation,

the nano column structure in LSMO and LMO films on the LAO substrate cannot be found, because of smaller misfit energy between the films and substrates.

Comparing the LSMO with LMO on the LAO, LSMO films were better than the LMO films, because Sr doping in the LMO decreased the lattice constant and the misfits of LSMO thin films became smaller. This result agreed with the theoretical results. In available literature, we cannot find deposited single crystal LSMO and LMO thin films on LAO using RF sputtering.

5.6 Magnetic Properties

(Data Provided by Varad)

The magnetic properties of LMO films were tested on vibration sample microscope at room temperature under -2000-2000 Oe applied field range. The typical hysteresis loop can be shown as follows which indicates that the all the films were paramagnetic in nature with very little magnetic moment.

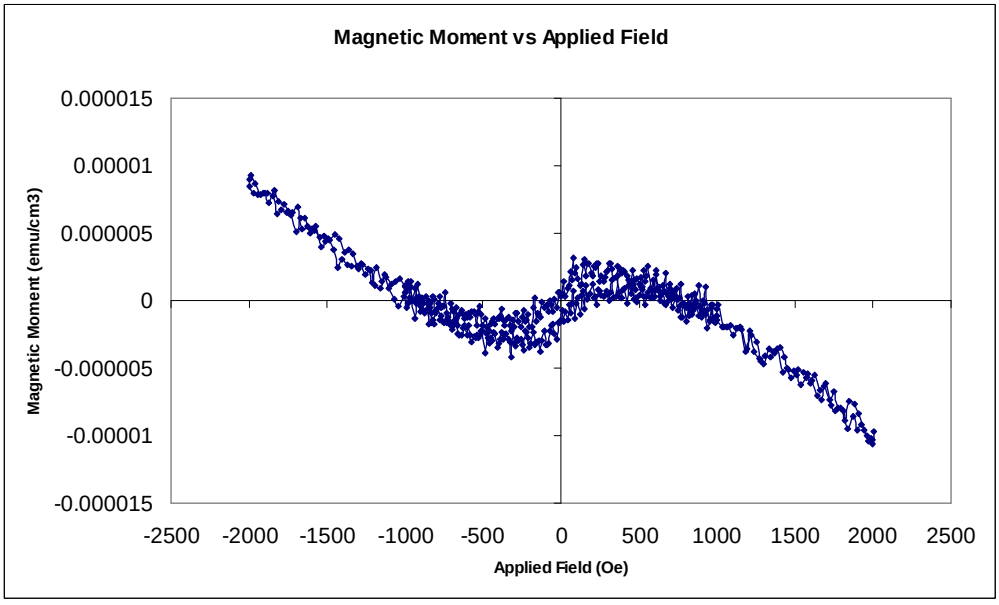

Figure 5.36 Typical hysteresis loop obtained from a sample at room temperature.

The magnetic properties of LMO were studied with SQUID in the temperature range of 10-100 K. The hysteresis loops obtained at 10K and 100K temperatures for each sample showed that the magnetic properties are dependent on the temperature. Polycrystalline sample LMO-S

shows a phase transition at 140 K and that of epitaxial LMO films deposited on LAO and MgO shows phase transition at 150K and 160 K respectively. The magnetic moment per unit volume of LMO grown on MgO is higher at 10K and 100K than that of the other sample.

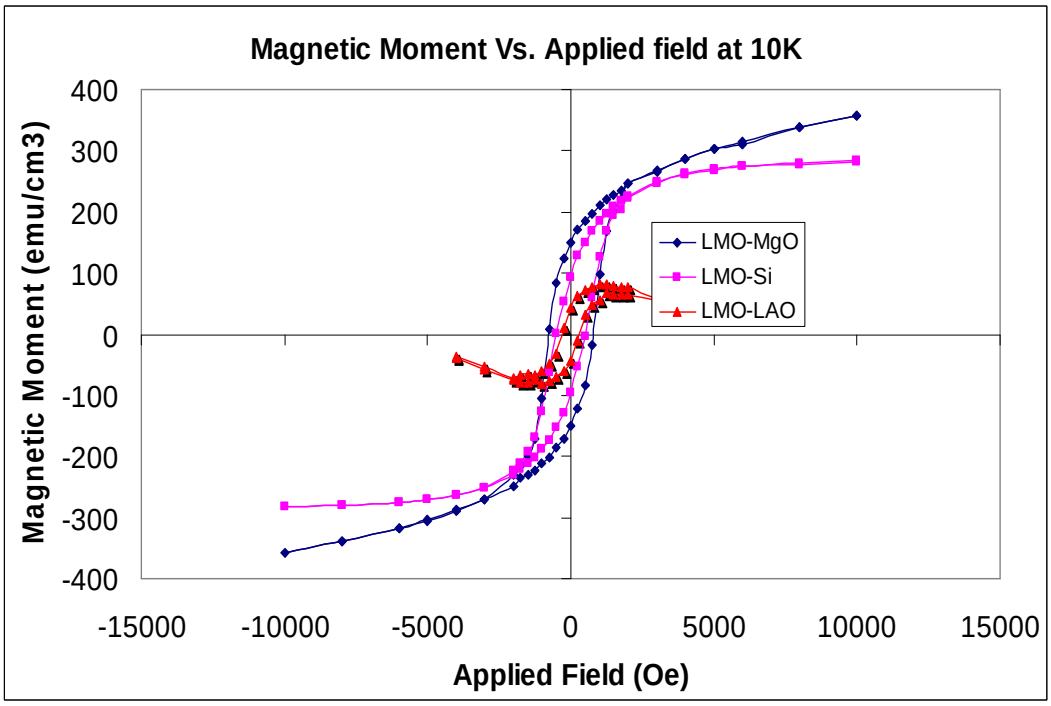

Figure 5.37 Hysteresis Loop for LMO thin films deposited on Si, MgO and LAO at 10K

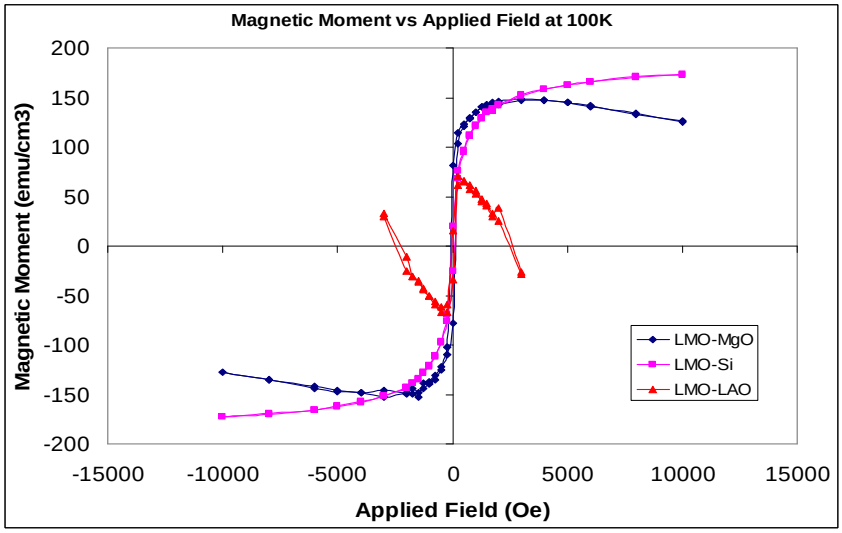

Figure 5.38 Hysteresis Loop for LMO thin films deposited on Si, MgO and LAO at 100K

According to the analysis of the above data, it is very clear that at low temperature, the sample has stronger magnetic strength. It is possible that the lower temperature reduces the thermal fluctuation of the ferromagnetically coupled Mn ion.

5.7 EDS Analysis (Data provided by Varad)

Elemental stoichiometry of LMO film was analyzed by Energy Dispersion X-ray (EDS) in connection with Hitachi SEM. Only the La: Mn ratio was evaluated for the LMO film, because of the oxygen always present in the substrate, it is impossible to measure the oxygen content on the film using EDS. Table 5.1 shows that the La: Mn ration was also 1:1. This result partially confirms that the materials of the target are congruently transferred to the films.

Table 5.2 Composition of the selection LMO sample

Films	EDS Analysis at. %		
	La	Mn	Other
LMO-Si-1	1.39	1.39	74.13 Si 23.13 O
LMO-Si-2	1.44	1.43	72.26 Si 24.88 O
LMO-Si-3	1.49	1.43	74.20Si 22.88O
LMO-MgO	0.66	0.64	42.83Mg 58.89O

CHAPTER 6

CONCLUSIONS

Polycrystalline and epitaxial single crystal lanthanum manganite thin films were successfully fabricated by RF magnetron sputtering method on Si (100), MgO (100), and LAO (100) substrates. LMO film on Si deposited at 750 °C showed nano column pervoskite type polycrystalline structure and films deposited at 700 °C are amorphous in structure. Therefore, substrate temperature is an important factor to determine film crystal structure. High temperature of substrates will enhance the mobility of atom on arrival and increase the rate of crystalline and at the same time it reduces the rate of solidification. Under the same deposition condition at 750°C, 30 W, 10mTorr, LMO films on Si with misfit of about -28.00% exhibited nano columnar polycrystalline structure, films on MgO with misfit of about -7.12% exhibited epitaxial crystal structure with column structure, and films on LAO with misfit of about 3.17 exhibited non columnar single crystal structure. Thus, the strain energy arising from misfit between the films and substrate causes the nano columnar formation.

Comparison of LSMO thin films on MgO with films on LAO deposited at 750°C 30 W, 10 mTorr shows that both the LSMO films on MgO and LAO substrate are epitaxial single crystal structures, LSMO films on MgO with misfit about -7.6% have nano columnar but LSMO on the LAO do not have columnar single crystal structure. We can infer that strong tensile stress lead to the nano columnar structure. Tensile stress of substrate cause the formation of the nano columnar and compressive stress of the substrate can't produce the nano columnar structure.

LSMO and LMO films on MgO are orthorhombic single crystal structures and the LSMO films are one domain orthorhombic structure and LMO films on LAO are cubic single crystal structure.

REFERENCES

1. F.L. Tang, M. Huang, W.J. Lu and W.Y Yu, Structural Relaxation and Jahn–Teller Distortion of $LaMnO_3$ (0 0 1) Surface, Surface Science, 603(2009) 949-954
2. J.C Jiang and E.I. Meletis, Nanofabrication of Self Organized ,Three Dimensional Epitaxial Oxide Nanorods, Thin Solid Films, 89(2005) 324
3. J. F. Mitchnell, D.Nargyriou, CD potter, D.J. Hinks, J.D Jorgensen, Phys. Rev. 54, (1996) 6172
4. Patrick Herve, Tchoua Ngamou, Naoufal bahlawane, Chemical Vapor Deposition and Electric Characterization of Perovskite Oxides La*M*O_3 (*M*=Co, Fe, Cr and Mn) Thin Films, Journal of Solid State Chemistry,182(1996) 849-854
5. Jeroen Van, Den Brink, Double Exchange via Degenerate Orbital, Physical Review Letters, 82 (2000)336
6. J.C Jiang, E.I. Meletis, Self Organized, Ordered Array of Coherent Orthogonal Column Nanostructures in Epitaxial LSMO Thin Film, Applied Physics Letters, volume 80(2000),4831
7. J.C Jiang and E. I. Meletis, Composition and Growth-Temperature Effect on the Microstructure of Epitaxial LSMO thin film on (100) LAO, Materials Research Society, Vol. 18,(2003)2556.
8. W. Cheikh-Rouhou, Koubaa, Journal of Magnetism and Magnetic Materials, 316 (2007) e648-e651
9. V. Sedykh, G. E. Abrosimoova, V. SH. Shekhtman, Features of Nanostructure in LMO, Material Letter, 63 (2009) 454-456.

10. Seung –Iel park, Ji-Hee Son, Magnetoresistive and Magnetic Properties of RF-Magnetron Sputtering Deposited La Ca, Sr-Mn-O Films, IEEE Transactions on Magnetic, Vol.36.No 5 September (2000).2933
11. YU Garbenko, OV. Melnikov, Preparation and Properties of $LaAgMnO_3$ Thin Film Epitaxial Films, Thin Solid Films, 516 (2008) 3783-3790
12. Q. Huang, J. W Lynm, Temperature and Field Dependence of the Phase Separation, Structure, and Magnetic ordering in $LaCaMnO_3$, Physical Review B,Vol.61, April (2000)8895
13. S. S. Wang, K. Wu, k. SHI, Development and Evolution of Biaxial Texture of Rolled Nickel Tapes by Ion Beam Bombardment for High T_c, Physic C, 407 (2004) 95-102
14. Kyung-Ku Choi, Tomoyasu Taniyama and Yohtaro, Room Temperature and Low-Field Magnetroesistance of La-Sr-Mn-O Thin Films IEEE Transactions On Magnetic, Vol. 35, No. 5,Sept.(1999) 2844
15. L. Hong, A. K. Soh, Y.C SONG Interface and Surface Effects on Ferroelectric Nano-Thin Films, Act Material, 56(2008)2966-2974
16. A. GaKi, O. Anagnostaki, D. Kiupis, T. Perrak, Optimization of $LaMO_3$ (M: Mn, Co, Fe) Synthesis through the Polymeric Precursor Route, Journal of Alloys and Compounds 451(2008)305-308
17. J. C. Jiang, W. Tian, Effects of Miscut of the $SrTi_{O3}$ Substrate on Microstructures of the Epitaxial $SrRu_{O3}$ Thin Films, Materials Science and Engineering B, Vol.5 (1998) 152-157
18. Lei Miao Ping Jin, Sputtering Deposition of Polycrystalline and Epitaxial TiO_2 Films with Anatase and Rutile Structures, 8th International Conference on ELECTRONIC Materials
19. W. Cheikh-Rouhou Koubaa, Effects of Silver Doping upon the Physical Properties of $LaSrAgMnO_3$ Manganese Oxide, Journal of Magnetism and Magnetic Materials, 316(2007)648-651
20. Leandro da Conceicao, Nielson F.P Ribera, Effect of Propellant on the Combustion Synthesized Sr-doped LMO Powders , Ceramics International, 35(2000) 1683-1687

21. M.-j. Casanove, C. Roucau, P Baules,Growth and relaxation mechanisms in LSMO Manganites deposited on $SrTiO_3$ (001) and MgO (001), Applied Surface SCIENCE 18 8(2002)1923
22. H.Okamoto, M.Karppinen, H. Yamaauchi, High-Temperature Synchrotron X-ray Diffraction Study of $LaMn_7O_{12}$, Solid State Science, (2009) 1-5
23. M. Dine EI Hannani, First-principles Investigations of Structural, Electronic and Magnetic Properties of Cubic LMO, Material Science in Semiconductor Processing
24. Guoyan Huo, Dayong Song, Structure, Magnetic and Electrical Transport Properties of the Perovskites $SmCaFeMnO_3$, Ceramics International, 34(2008)497-503
25. N. Fujihira, T.SEI and T. TSUCHIYA, Preparation and Properties of Highly Conductive $La_{1-X}M_XMnO_3$ Thin Film Showing Magnetic Effect from Sol-Gel Process, Journal of Sol-Gel Science and Technology, 4135-140(1995)134
26. H.S Kim, S. S. Oh, H.S. Ha, Deposition of LMO Buffer Layer on IBAD-MgO Template by Reactive DC sputtering, Physics C, 469(2009)1554-1558
27. Brendan J. Kennedy, Jimmy Ting, Qing Di Zhou, Structural Characterization for the Perovskite Series $SrCaCeMnO_3$ Influence of the Jahn-Teller Effect, Journal of Solid State Chemistry, 182(2009)9564-959
28. G. Y. Wang, S.W. Liu, T. Wu, Phase Separation Induced by Oxygen Deficiency in $LaCaMnO_3$ Thin Films, Solid State Communications, 144(2007)454-495
29. A.A Dakhel, DC-conduction Mechanism in Lanthanum-Manganese Oxide Films Grown on P-Si substrate, Microelectronics Reliabiltiy, 48(2008)395-400
30. Yohei, Kashiwada, Hiroyuki Fujishiro, Metal Insulator Transition and Phonon Scattering Mechanisms in $La_{1-X}Sr_xCoO_3$,Physics B,378-380(2006)529-531
31. F. L. Tang, M. Huang, W. L. Lu, Structure Relaxation and Jahn-Teller Distortion of LMO (001) Surface, Surface Science, 603 (2009) 949-954

BIOGRAPHICAL INFORMATION

Yin sheng Fang was born on Jan 1 1971 in China. In 1998, he graduated with a Bachelor of Science in Material Science and Engineering in Jinan University. Since 2008, he started to study Master Degree in Material Science and Engineering at University of the Texas at the Arlington. Currently, his research area focuses on the microstructure of perovskite –type ceramic material using Transmission Electron Microscopy. He is a candidate for the degree of Master of Science in Material Science and Engineering.